1981

The response and the lift force analysis of a cylinder oscillating in still water

Youn-sik Park
Iowa State University

PARK, YOUN-SIK

THE RESPONSE AND THE LIFT FORCE ANALYSIS OF A CYLINDER OSCILLATING IN STILL WATER

Iowa State University PH.D. 1981

PLEASE NOTE:

In all cases this material has been filmed in the best possible way from the available copy. Problems encountered with this document have been identified here with a check mark __√__.

1. Glossy photographs or pages _____
2. Colored illustrations, paper or print _____
3. Photographs with dark background _____
4. Illustrations are poor copy _____
5. Pages with black marks, not original copy _____
6. Print shows through as there is text on both sides of page _____
7. Indistinct, broken or small print on several pages ✓
8. Print exceeds margin requirements _____
9. Tightly bound copy with print lost in spine _____
10. Computer printout pages with indistinct print _____
11. Page(s) _____ lacking when material received, and not available from school or author.
12. Page(s) _____ seem to be missing in numbering only as text follows.
13. Two pages numbered _____. Text follows.
14. Curling and wrinkled pages _____
15. Other _____

The response and the lift force analysis of a cylinder oscillating in still water

by

Youn-sik Park

A Dissertation Submitted to the
Graduate Faculty in Partial Fulfillment of the
Requirements for the Degree of
DOCTOR OF PHILOSOPHY

Department: Engineering Science and Mechanics
Major: Engineering Mechanics

Approved:

Signature was redacted for privacy.

In Charge of Major Work

Signature was redacted for privacy.

For the Major Department

Signature was redacted for privacy.

For the Graduate College

Iowa State University
Ames, Iowa

1981

TABLE OF CONTENTS

I. INTRODUCTION

In recent years flow-induced vibration problems have become increasingly important. Designers are using materials to their limits building structures to become progressively lighter and more flexible.

In the past two decades a great deal of research work has been done, especially on fluid-structure interaction problems. The ultimate question of all those research works can be summarized as what happens to the structure and to the fluid flow when a structure is exposed to a fluid flow. The previous research work can be divided into three categories, depending upon viewpoints. These are: i) exploring the behavior of structures due to surrounding fluid flow, ii) exploring the behavior of the fluid flow around structures, and iii) exploring the relationship between structure and surrounding fluid flow interaction.

Exact knowledge of a structure's behavior due to surrounding fluid flow is very important in designing bridges, antennas, off-shore structures, heat exchangers, undersea cables,...etc. since large amplitude structural vibrations can cause a destructive effect.

Many research studies have been done to determine and predict the fluid in-line forces acting on a cylinder in steady and oscillating fluid flow. Almost all of those

studies have been based on the Morison equation [1], where the two in-line force components of drag and inertia are identified, and the equation tries to relate these forces to the velocity and acceleration of the fluid particles. Besides the in-line forces, the so-called lift force plays an important role in determining the behavior of a cylinder due to fluid flow. Lately, it was found that in some situations the lift force is as large as or larger than the in-line forces [2]. Furthermore, in the opinion of some people the lift force is more important than the in-line force; not only because of its magnitude, but also because of its frequency, which under some circumstances may cause resonant motion of the structure. The neglect of such vibrations may lead to serious cracking and consequent failure of the structural members due to fatigue.

It should be apparent that our ability to estimate the fluid forces, including both in-line and lift forces, and the resulting structural response is critical in designing structures exposed to fluid flow. Vortex shedding is the dominant mechanism for structures exposed to steady flow. This mechanism can be described simply as follows for a bluff cylinder. As a fluid particle flows toward the leading edge of a bluff cylinder, the pressure rises from the free stream pressure to the stagnation pressure. The high fluid pressure near the

leading edge impels the developing boundary layers about both sides of the cylinder. However, the pressure forces are not sufficient to force the boundary layers around the back side of bluff cylinders at high Reynolds numbers. Near the widest section of the cylinder, the boundary layers separate from each side of the cylinder surface and form two free shear layers that trail off in the flow. These two free shear layers bound the wake. Since the intermost portion of the free shear layers moves much more slowly than the outermost portion of the layers which are in contact with the free stream, the free shear layers tend to roll up into discrete, swirling vortices. Thus, a regular pattern of vortices is formed in the wake. The vortex sheddings which are alternately generated from each side of the structures lead to the periodic lift forces on the structures. The so-called Strouhal number is used to relate the vortex shedding frequency, the cylinder diameter, and the free stream velocity.

The relationship between the structural responses and the vortices in the fluid flow have been investigated by several researchers. In certain cases, it was found that a locked-on phenomenon occurs. In the locked-on phenomenon the vortex shedding frequency adheres to the structural response frequency around the natural frequency of an elastic structure. In other words, under certain

operating conditions, the response affects vortex formation and vice versa. Also, it was observed that the locked-on phenomenon increases the vortex shedding strength and, consequently, causes large structural responses in the elastic structure. This locked-on phenomenon can be observed in both steady and oscillating fluid flow around the structure.

Several attempts have been made to develop analytical models to predict fluid forces and structural responses. It would be desirable to analytically predict the fluid forces and the cylinder responses using cylinder surface pressures obtained from an analysis of the fluid flow field. Ideally, one would solve the time-dependent Navier-Stokes equations in the presence of the vibrating cylinder. The flow separation and vortex formation would emerge naturally from the calculated solution. The resulting pressure and shear forces acting on the cylinder surface would provide the forcing function. These forcing functions are then used to predict cylinder structural motion and the calculations are repeated. Solutions of this type have been limited to either stationary cylinders at Reynolds numbers below 1,000 where the flow is laminar or to solutions where viscosity has been neglected. A general integrated analysis of both the flow fluid and the cylinder motion is not available for nearly all practical cases. Therefore,

only limited models have been developed to describe the cylinder-fluid interaction.

The limited models introduced up to the present are the "wake oscillator model" [3, 4] and the "correlation model" [3, 5, 6]. These models do not solve the time dependent Navier-Stokes equations. They do, however, incorporate many of the dynamic effects that have been observed experimentally.

Both models are not rigorous approximations of the fluid-structure interactions. Nevertheless, they have proven useful for estimating the structural response of circular structural components when exposed to steady fluid flow.

In the case of oscillating fluid flow, the flow characteristics are much more complicated than in steady flow. In this case, the fluid travels over the cylinder wake, creating a fluid flow pattern difficult to analyze.

Up to this moment, no theoretical model can predict the forces and corresponding structural responses of a circular cylinder exposed to a periodic fluid flow. However, there are relatively many experimental studies of the forces acting on stationary cylinders compared to the number of experimental studies on the complex dynamic responses of elastically mounted structures placed in oscillating flows.

Recently there has been growing interest in the fluid-structure interactions when the fluid flow is periodic. This interest is motivated by the practical needs to build optimum off-shore structures. The interactions between fluid and structures can cause serious damage to the structure since the wave loads can easily exceed the expected value predicted by current information. Many investigators have tried to estimate reliable wave loads. Keulegan and Carpenter [7], Sarpkaya [8, 9], Hamann and Dalton [10], Garrison, Field and May [11], etc. have measured fluid forces on a cylinder exposed to an oscillating fluid flow. Of these investigators, Sarpkaya [9] did the most systematic studies where the fluid in-line and lift forces were measured over the wide range of Reynolds numbers. He concluded that for oscillating fluid flow, the fluid forces are strongly related with the period parameter (Keulegan-Carpenter number) as well as the Reynolds number.

All the above studies for oscillating fluid flows were performed for a stationary cylinder. But in case of elastically mounted cylinder, the cylinder responses affect the fluid forces and responses.

In this study, the fluid lift forces and the cylinder responses due to an oscillating fluid flow were measured experimentally. The corresponding analysis placed emphasis

on the prediction of fluid lift forces and cylinder responses normal to the deterministic, sinusoidal oscillating flow.

It is the author's belief that the fluid lift forces are affected by the cylinder vibrations. Consequently, the fluid force estimation based on stationary cylinder data must be in error compared to the actual situation.

For the experiments described in the research reported herein, the elastically mounted cylinder motion relative to the global fluid motion can form a closed Lissajous loop as shown in Figure 1. A locked-on phenomenon occurs in this case where the vortex shedding frequency (f_v) and the structural natural frequency (f_n) are related to the oscillating fluid frequency (f_d) in an integer manner. This locked-on phenomenon causes an increase in the lift force due to increased strength of vortex shedding from the same side of the cylinder; i.e. the correlation of shedding from a given side of the cylinder is increased. It is also helpful to visualize the vortices to be "trapped" within the Lissajous path as seen in Figure 1. Note how the cylinder moves naturally around the "trapped vortices," reinforcing the vortices on each pass. As the input motion amplitude (A) increases there is more time for the vortices to dissipate and move out of the pattern before the cylinder returns. Consequently, the amplitude of response decreases

and this simple pattern of behavior begins to break down, giving smaller amplitudes of motion (B). It was known that the maximum value of B is about one cylinder diameter peak to peak for a steady fluid flow. For an oscillating fluid flow the maximum value of B was measured slightly more than one cylinder diameter (1.0D ~ 1.15D) peak to peak. While the above description is helpful in visualizing the maximum response case, the case of periodic flow about an elastically mounted cylinder involves a complex interaction.

The relationship between the cylinder natural frequency (f_n), the structural response frequency (f_r), the vortex shedding frequency (f_v) and the fluid oscillating (wave) frequency (f_d) is more important in determining fluid forces and structural response than the conventional non-dimensional parameters described by Reynolds and Keulegan-Carpenter (Period parameter) number. It will be seen that this apparently radical departure from conventional practice for presenting experimental results leads to an integrated picture of fluid-structure interaction that includes both elastically and rigidly mounted cylinders.

II. REVIEW OF LITERATURE

The study of fluid-structure interaction problems started with vortex shedding phenomenon behind a bluff body. The first recorded observation of the phenomenon is credited to Leonardo da Vinci, who sketched a row of vortices in the wake of a bluff body in a stream in the fifteenth century.

In 1878, Strouhal made a quantitative study of vortex shedding. He found that the tone frequency (f_v) generated by a taut wire in an airstream was a function of the wire diameter (D) and the airstream velocity (U). He introduced the famous Strouhal number (S_t) which is commonly used today to study the vortex shedding frequency; i.e. $S_t = \frac{f_v D}{U}$.

In 1879, Lord Rayleigh proved that the rate of vortex shedding, f_v, was a function not only of fluid velocity and cylinder diameter but also of Reynolds number. A number of more recent researchers have confirmed the general results of Rayleigh's work and have succeeded in defining the Strouhal number-Reynolds number dependence.

In 1908, Bernard showed that the vibration of the wire noticed by Strouhal and Lord Rayleigh was related to the formation of two rows of nearly parallel vortices in the wake.

In 1912, Von Karman analyzed the formation of a stable street of staggered vortices behind a fixed circular cylinder in a uniform flow.

Many studies have been made in the last two decades. These are best presented in several categories, based upon the experimental approach as well as the type of fluid-structure interaction problem.

It is important to distinguish between data obtained from rigidly mounted cylinders as opposed to those which are elastically mounted and free to interact with the fluid.

A. Fluid Forces in a Uniform Flow

Many investigators have examined fluid forces acting on a rigid or a vibrating circular cylinder in a uniform fluid flow. Usually the fluid forces can be divided into two terms. One is in-line force which acts parallel to the direction of fluid flow and the other is lift force acting perpendicular to the fluid flow. Most of the former studies related lift force with vortex sheddings behind a circular cylinder and examined in-line force using the Morison equation [1] which is given by:

$$F_{IN} = 0.5C_d LD\rho|U|U + 0.25\pi\rho LD^2 C_m \frac{dU}{dt} \qquad (1)$$

where C_d is the drag force coefficient, C_m is the inertia force coefficient, D is the cylinder diameter, U is the uniform fluid velocity, ρ is the fluid density and L is the cylinder length immersed in fluid. As shown, the Morison equation consists of two in-line force terms (drag and inertia).

Bishop and Hassan [12] measured the in-line and lift forces on both forced and naturally induced vortex vibrating cylinder in uniform fluid flow.

Tanida, Okajima and Watanabe [13] measured the in-line and lift forces in uniform flow on an elastically mounted cylinder at Reynolds numbers from 40 to 1×10^4 and investigated the stability of the oscillating cylinder. They also observed the locked-on phenomenon.

Fung [14] measured the lift and in-line forces on a rigid cylinder in an incompressible uniform fluid flow at supercritical Reynolds numbers ($R_e > 1 \times 10^5 - 5 \times 10^5$). The results were plotted in terms of the power spectral densities, since the measured forces were random in nature. It was found that the forces decreased with increasing Reynolds number, in agreement with other experimental results.

Batham [15] investigated fluid forces by measuring pressure distributions on circular cylinders having smooth and rough surfaces at Reynolds numbers of 1.1×10^5 to

2.4×10^5. He found that the cylinder surface condition plays a very important role for the pressure distribution and, consequently, the fluid forces in the critical Reynolds number region.

Griffin and Ramberg [16] measured the vortex strength and spacing in the wake of a vibrating cylinder, and used the Von Karman drag formulation to determine the drag force. The force values determined in this manner were in agreement with direct force measurements made under similar flow conditions.

Toebes [5] studied the lift forces acting on an elastically mounted cylinder in uniform fluid flow by measuring fluid velocity and pressure near the cylinder surface for Reynolds number up to 1×10^5. He also investigated the effect of the cylinder vibrating motion on the fluid velocity and corresponding cylinder surface pressure distribution. It was observed that when the cylinder vibrating frequency is near a multiple or submultiple of the vortex shedding frequency, vortex strength is increased and the phase differences in vortex formation are decreased.

Sarpkaya [17] also measured fluid lift and in-line forces on a circular cylinder forced to vibrate in a uniform flow. He observed that the in-line force increases as the vibration amplitude increases and the lift force

coefficient scatters significantly when the excitation frequency is in the vicinity of the Strouhal frequency.

King, Prosser and Johns [18] investigated the nature of flow-induced oscillations of circular cylindrical model piles that were typical of full-scale marine structures. They examined the first and the second mode of free-ended cantilever oscillations.

Weaver [19] studied wind-induced vibration on an elastic cylinder due to vortex sheddings in wind-tunnel tests. He introduced various methods of reducing the flow-induced forces on circular cylinders. He insisted that by wrapping spoiler wires around the cylinder, the coherence of the shedding could be reduced and subsequently the flow-induced forces could also be significantly reduced.

Silvio [20] studied the flow-induced vibration and the vortex shedding frequency when an elastically mounted cylinder was exposed to a steady flow. He observed the locked-on phenomenon and found that as the amplitude of the cylinder response increases, there is a corresponding reduction of the vortex shedding frequency. In other words, he observed decreasingly vortex shedding frequency around a locked-on region. This observation is in agreement with Griffin's results [21].

In all of the above mentioned literature, the authors tried to analyze the complicated fluid-structure interaction

problems in terms of measured fluid forces and/or structural responses. On the other hand some investigators have tried to establish some kind of theoretical model to predict the fluid forces and correspondingly structural responses.

Landl [22] introduced a mathematical model for flow-induced vibrations of a circular cylinder in uniform flow field using fifth order damping terms. He tried to explain the experimental data using his model. He succeeded in qualitative descriptions but failed to obtain quantitative results.

The nature of self-excited vortex shedding suggested that the fluid behavior might be modeled by a simple, nonlinear oscillator as first suggested by Bishop and Hassan [12]. This idea has been pursued by Hartlen and Currie [23], and Skop and Griffin [24], who have devised models in which the cylinder lift coefficient satisfies a Van der Pol type equation. Hartlen and Currie [23] confirmed that this wake oscillator model idea is helpful in determining the motion of an elastically mounted cylinder and the lift force on an externally driven cylinder in an uniform fluid flow field.

Iwan and Blevins [4] suggested a wake oscillator model to estimate the responses of an elastic cylinder by analyzing a control volume consisting of the cylinder and several vortices in the wake. The corresponding

analysis using fluid mechanics techniques lead to the formulation of a nonlinear differential equation. Model parameters were determined by curve-fitting experimental results for stationary and forced cylinders. They found that their model is capable of predicting the responses of elastic cylindrical structures in uniform fluid flow in the Reynolds number range of 1×10^3 to 1×10^5.

Blevins and Burton [6] established a semi-empirical dynamic model for investigating the fluid forces induced on a bluff cylinder by vortex shedding using a random vibration theory. They applied the model to determine the forces exerted on elastic cylinders at resonance with vortex shedding. The predictions are in good agreement with experimental data.

B. Vortex Wake Studies

Several investigations have been concerned with the fluid wake behind a circular bluff cylinder. These studies are reviewed here.

Roshko [25] studied the pressure distribution in the wake of a rigid cylinder in a uniform fluid flow and found that the addition of a splitter plate on the downstream side has a dramatic effect on the pressure distribution. He concluded that the flow field in the wake of a bluff body is determined almost entirely by the vortex formation

region contained in the first four or five cylinder diameters downstream of the body.

Stansby [26] studied the frequencies of vortex shedding from circular cylinders forced to oscillate transversely in low-turbulence uniform and shear flows. In both flows the vortex shedding frequency locked-on to the cylinder vibrating frequency and to submultiples of the cylinder frequency.

Koopman [27], Griffin [28] and Griffin and Ramberg [29] used flow visualization methods to observe the vortex patterns in the wake of cylinder oscillated perpendicular to the flow. These studies were made in an attempt to determine the interaction between the structure and the fluid when a locked-on condition existed. It was found that a locked-on condition occurred when the drive frequency was within $\pm$ 20 per cent of the vortex shedding frequency.

Griffin and Ramberg [30] studied the wake of a stationary and a vibrating cylinder to the in-line direction in steady air flow. They found that the results obtained in the air stream are in agreement with previous findings from free and forced vibration experiments in water at both higher and lower Reynolds numbers.

Ogawa and Nakagawa [31] studied the stability condition of a vortex street behind a bluff cylindrical body

and obtained the vortex shedding stability criterion for stationary and vibrating cylinders.

Griffin [21] measured the pressure and fluid velocity at the separation point. Using the experimentally obtained parameters, he derived a model for a universal wake Strouhal number, valid in the subcritical range of Reynolds numbers for both forced and vortex-excited oscillations in the locking-on region. The Strouhal numbers thus obtained are constant at $S_t = 0.178$ over the range of wake Reynolds numbers $Re = 700$ to 5×10^4. This model is in good agreement with the results obtained by Roshko [25] and Bearman [32] for stationary circular cylinders and other bluff bodies in the same range of Reynolds numbers.

C. Fluid Forces in Oscillating Fluid Flow

The optimum design of large offshore structures requires accurate hydrodynamic data on fluid forces and the corresponding structural response. The urgency for this information grows as larger and larger structures are being used for energy and mineral production from the bottom of the sea. Ideally, full-scale ocean tests should give realistic wave loads on the structure. Various studies have been conducted to determine the drag and inertia coefficients by instrumenting full-sized piles subjected to ocean waves. While these large-scale tests

have probably resulted in the most acceptable data to the present, they are nevertheless very limited. No control may be exercised over the incident wave in such tests. Therefore, one can not hope to correlate the results with the properties of the incident wave in a precise manner. The irregular wave motion encountered is, of course, complex and does not lend itself to description through a simple dimensionless parameter.

For this reason the question of the value of in-line and lift force coefficients for use in calculating wave loads on cylindrical members has endured many years. Neither laboratory wave channel tests nor full-scale ocean tests have resulted in very much systematic information as well as a full understanding.

However, several investigators have collected data for estimating wave loads of off-shore structures from full-scale ocean tests. Fairly complete wave force data can be found in Wiegel [33], Hogben [34], and Grace [35] While the nature of the wave motion is very random, Moe and Crandall [36] attempted to estimate the extreme wave forces on a fixed cylindrical pile in a random sea-state by using statistical techniques. They assumed that the wave force follows the Morison equation.

As mentioned above, many investigators have used laboratory experiments rather than full-scale ocean tests to obtain adequate control of input wave motion properties.

Keulegan and Carpenter [7] were the first to undertake the question, "What is the force acting on a circular cylinder in two dimensional flow oscillating with simple sinusoidal motion?" They placed a circular cylinder at the node point of a standing wave so that the fluid motion at the location of the test cylinder was sinusoidal and in the horizontal direction only. The force was expressed in terms of the fluid velocity and acceleration according to the well-known Morison equation and the coefficients of drag and inertia obtained from the experiments were plotted against the period parameter, $U_m T/D(=2\pi A/D)$, in which U_m denotes the amplitude of the sinusoidally varying velocity; T denotes the period of the wave motion; D denotes the cylinder diameter; and A denotes the amplitude of the oscillating wave motion. They recognized the possibility of Reynolds number dependence of the drag and inertia coefficients as well as the period parameter dependence. They found that no such correlation with Reynolds number, in fact, existed. Nevertheless, as will be examined subsequently, a replot of their data that spans the 7,000 to 30,000 Reynolds number range clearly indicates to the

contrary that both coefficients are rather strongly Reynolds number dependent.

It is suspected that the Reynolds number dependence was overlooked because of the fact that the experimental apparatus used by Keulegan and Carpenter was not well-suited to the study. Each time the period parameter was changed the Reynolds number also changed so that it was impossible to carry out a series of tests with varying Reynolds number with a fixed value of the period parameter without changing the test cylinder diameter each time. In addition, the range of Reynolds numbers encountered was very limited and in this limited range the coefficients underwent some rather unexpected variations that were apparently interpreted as scatter.

Sarpkaya [8] carried out tests similar to Keulegan and Carpenter in a similar Reynolds number range using a U-tube oscillator in place of a standing wave oscillator. In this study again, the absence of any systematic Reynolds number dependence was emphasized. The results, that were plotted in the form of the drag and inertia coefficients versus the period parameter, were generally similar to those of the Keulegan and Carpenter study.

Garrison, Field and May [11] studied the effect of both the Reynolds numbers and the period parameter dependence of the drag and inertia coefficients in an oscillating flow.

They oscillated the cylinder in still fluid rather than oscillating the fluid in order to get strict control of both parameters. They calculated the drag and inertia force coefficient for large values of the Reynolds numbers and period parameters and confirmed the fact that force coefficients are strongly dependent on both parameters.

Hamann and Dalton [10] measured the in-line forces directly acting on a circular cylinder due to oscillating fluid flow. They related the measured forces with the fluid velocity and acceleration instead of plotting against Reynolds number and period parameter. They observed that the fluid forces during acceleration are different than those in deceleration. This phenomenon is in agreement with the observation of Laird, Johnson and Walker [37]

As in the case of uniform fluid flow around a circular cylinder, the vortex shedding behind a cylinder generates lift forces in the oscillating fluid flow cases as well. But in the case of oscillating fluid flow, the flow pattern around a circular cylinder is much more complicated than in the uniform flow case. In the oscillatory case the cylinder is subjected to its own wake when fluid flow reverses direction. This process of being subjected to its own wake occurs over and over.

Several researchers have investigated the lift forces acting on a circular cylinder in periodic fluid flow.

Bidde [38] directly measured in-line and lift forces acting on a fixed cylinder due to wave motion around the cylinder. He examined the ratio of lift to in-line forces and found that the period parameter appears to be useful in predicting the ratio (lift to in-line forces) and also insisted that the lift forces are as important as the in-line forces. He noticed that the lift forces are important not only because of their magnitude, but also because of their frequency, which under some circumstances may cause resonance motion of the structure, with possible disastrous consequences. This occurs even when the wave frequency is much lower than the structure's natural frequency.

Sarpkaya [8] also measured lift and in-line forces. He used a small size U-shaped vertical water tunnel instead of a water channel. He noticed the importance of the lift forces after considering the magnitude of frequencies of the lift forces. He concluded that the lift force is as large as or larger than the in-line force in a certain range of the period parameters.

Almost all of the fluid forces data obtained in laboratory studies are for Reynolds numbers generally two to three orders of magnitude smaller than prototype full-size structure Reynolds numbers. This happens because there are many limitations in obtaining large Reynolds

numbers in a laboratory test. As there has been a growing awareness that the coefficients obtained at relatively low Reynolds numbers may not be applicable at higher Reynolds numbers, Sarpkaya [9] built a giant structure to obtain data for prototype Reynolds numbers with strict parameter control. He collected a lot of information about the fluid force coefficients in oscillating flow and confirmed his previous work (reference [8]).

While studying fluid forces on a circular cylinder in the periodic fluid flow, it is natural to ask the question, "What happens when the circular cylinder in the oscillating fluid flow is elastically mounted in the direction perpendicular to the oscillating fluid?" How do the vortex sheddings affect the fluid lift forces and the correponsing cylinder responses, and conversly, how are the vortex sheddings affected by the cylinder motion? How does the natural frequency of the cylinder affect the cylinder responses? Unfortunately, at this moment, only a single reference could be found wherein the above questions were addressed for an elastically mounted cylinder subjected to an oscillating fluid flow. Wilson [39] attempted to obtain the lift force coefficient indirectly. He oscillated an elastically mounted small cylinder in still water and tried to measure fluid forces directly. Due to the high noise level compared with the fluid force signal, he

failed to obtain fluid forces directly. Then he measured the cylinder responses and using a wake oscillator type model, derived the lift force coefficient. He found that the period parameter is important to analyze the oscillating fluid problem and said that the lift force coefficient decreases with an increasing period parameter.

In this work, the fluid lift forces acting on an elastically mounted cylinder and the cylinder responses were measured directly. Also the vortex shedding frequency, the natural frequency of the elastically mounted cylinder, and the cylinder response frequency were extensively measured and examined for interrelationships.

III. EXPERIMENTAL WORK

A. Experimental Apparatus

The prediction of fluid dynamic forces exerted on bodies immersed in a viscous fluid has always presented problems of similarity and scale. As it often occurs, hydrodynamic force coefficients corresponding to large values of Reynolds number are needed in full-sized applications while it is difficult to produce such flows in smaller laboratory experiments. The problem of calculating wave forces on offshore structures, either floating or fixed, has the same handicap. Wave channel testing generally produces Reynolds numbers on cylindrical members on the order of 1×10^4 to 1×10^5 whereas values well beyond 1×10^6 are more common in full-sized applications. Wave channel testing is further handicapped by the fact that one generally does not have independent control over Reynolds numbers since Froude scaling is necessary. It is practically impossible to achieve both Reynolds and Froude similarity at the same time unless full-sized structures are tested. On the other hand, laboratory experiments give the chance for strict control of parameters not possible in some large scale testing. Consequently, the problem can usually be controlled and analyzed more easily using one or two nondimensional numbers than would be possible with a prototype. Strict parameter control is

more easily obtained in laboratory testing over full-scale prototype testing. Significant problem understanding can be obtained from cost effective laboratory tests. The results presented here were performed in a laboratory.

A special experimental apparatus was designed and built to measure fluid lift forces and cylinder responses due to periodic fluid flow.

There are two different ways to produce a relative periodic motion between a cylindrical model and the surrounding fluid. One method is to oscillate the fluid past a stationary cylinder while the other is to oscillate the cylinder past the stationary fluid. Kinematically there is no difference between the two situations when viewed from appropriate reference frames. But experimentally, there are immense differences in implementation between the two methods.

In the experiments described herein, the cylinder oscillating method was selected. Not only because of relatively simple implementation but also because of the fact that the cylinder oscillating method allowed the parameters involved to be easily and precisely varied over a wide range. On the other hand, it has three distinct disadvantages that need to be overcome. These are; 1) the effect of waves and free surface disturbances in the water tank created by the oscillating body are

difficult to assess, 2) the supporting structure and driving mechanism can transmit vibration disturbances to the fluid surface from sources such as the driving motor and speed reduction gear box, 3) the inertia force due to the mass of the oscillating body has to be subtracted from the measured force signal.

In this experiment, several ideas were implemented to overcome these difficulties. Soft and porous packing materials were used around the inside of the water tank to absorb surface disturbances and to reduce wave reflections from the wall. The unwanted high frequency supporting structure vibration signals were eliminated using low pass filters that were carefully designed not to distort, both the magnitude and the phase, the original signal. A unique technique [40] was developed to eliminate the inertia force due to the oscillating cylinder by installing two force transducers on the moving cylinder. The details about inertia force elimination were given in Appendix A. Using this technique, about 97 per cent of the unwanted inertia forces were removed from the force signal.

Figure 2 shows a schematic drawing of the experimental apparatus used in this work.

A strong unistrut structure (52 in. wide, 90 in. long, 84 in. high) was built and two flat moving plates (Plates A and B) are placed at the top side of the unistrut

structure. A variable speed motor drives the Plate A through a 10:1 speed reduction gear box. It was designed so that the driving amplitude of the Plate A can be continuously adjusted from 0 in. to 10 in. Then the motion of Plate A was transmitted to Plate B through cables which were connected between the two plates. The oscillation amplitude of Plate B can be magnified by a factor of two through use of four pulleys and two cables. In other words, by using four pulleys and two cables, Plate B can be given a harmonic motion with the same frequency but with twice the amplitude of Plate A. This fact gives a great advantage to reduce the size of the experimental apparatus. Plate C was built for mounting the force transducers and circular cylinder models with the dimensions of 19.5 x 19.5 x 3 in. Three thin aluminum flexure strips connected Plate C to Plate B. These aluminum flexure strips allowed Plate C to move relative to Plate A in the response direction (y-direction) while remaining relatively rigid in driving direction (x-direction).

A water tank was constructed with dimensions of 48 in. wide, 30 in. high, and 84 in. long and placed on the inside of the unistrut structure.

Two force transducers and a cylindrical model were placed on Plate C as shown in Figure 2.

The detailed specifications of the experimental set-up can be summarized as below.

1) The amplitude of the cylinder input oscillation motion, corresponding to wave motion, can be varied continuously from 0 in. to 20 in.
2) The driving frequency of the cylinder oscillation can be varied from 0.067 Hz to 0.67 Hz continuously.
3) The circular cylindrical model can be easily changed for testing different diameter sizes.
4) The cylinder model can be released or fixed in the response direction (y-direction) without difficulty.
5) The cylinder length immersed in the water can be adjusted by changing water depth in the tank.

Park [40] describes the experimental apparatus in great detail.

B. Electrical Measurements System and Calibration

As discussed in the introduction, this study needs to measure the fluid lift forces (F_L), the cylinder response motion in a direction perpendicular to the cylinder input direction (y), the natural frequency of the elastically mounted cylinder in the response direction (f_n), the cylinder input frequency (f_d) and the cylinder inertia

force (F_I) to eliminate inertia effects due to cylinder oscillation.

Before discussing the details of the measurement system, it is worthwhile to consider the desired output.

1) The input frequency of the driving mechanism (f_d) and the natural frequency of the system in the response direction (f_n). The input frequency could be monitored constantly during the experiments.
2) A time history record of the cylinder response in the y-direction (y).
3) A time history record of the fluid lift forces (F_L).

The block diagram of the measurement system used to provide the desired output information described above is shown in Figure 3. Each element for the output and the calibration information is briefly described below, and a complete schematic diagram of the circuitry is included in Appendix B.

A microswitch circuit was used to measure the input frequency (f_d). The microswitch (ACRO Electric Co., type BZ-2RL) was placed at one end point of the cylinder input motion so that for every back and forth input motion an on-off signal was generated. This on-off signal was conditioned by a Zener Diode Triggering Circuit which in turn was connected to a Hewlett Packard model HP528D frequency counter. The input frequency (f_d) was

consistently monitored during the experiment. The input frequency (f_d) could be maintained easily within 0.5 per cent error by adjusting the speed of the varidrive motor.

Four active 120 ohm straingages with a gage factor of 2.09 were used to measure cylinder responses in y-direction (y). These gages formed a standard four-arm wheatstone bridge and provided both high sensitivity and temperature compensation. This straingage bridge was connected to an amplifier and a low pass filter circuit.

The low pass filter circuit was used to eliminate spurious high frequency signals. It is known that two problems occurred with this filter circuit. The first is the phase shift while the second is amplitude attenuation of the signal. The filter circuit is a second order type so as to minimize the amplitude attenuation. The natural frequency and the damping ratio were carefully selected for the filter after considering the useful driving frequency range. Since the highest resonant frequency of the system was around 3 Hz. The natural frequency of the filter circuit was designed to be 7 Hz and a damping ratio of 0.65 was picked. This provided a roll off of 12 db/octave (40 db/decade) for frequencies above 10 Hz, a phase shift that was a linear function of frequency (within $\pm$ 5°), and the gain was unity $\pm$ 1.2 per cent below 3.5 Hz (when

$\frac{f}{f_n} = 0.5$). The filter used did not appreciably attenuate any of the desired signal in the frequency region of less than 3 Hz which is the useful frequency range in this experimental set-up. The linear phase shift allowed the signal to be reconstructed as the output without significant phase distortion.

The linearity and voltage sensitivity of this cylinder response measuring circuit was obtained using a dial indicator to measure known displacements in the y-direction. The output voltage from the strain gage circuit was recorded while increasing the cylinder responses in y-direction. A statistical analysis of the recorded calibration data gave a straight line calibration curve with a slope of 1.95 volt/in., a correlation coefficient of 0.9999, and a standard estimate of error of $\pm$ 8.85 mv (4.54×10^{-3} in.) for displacements less than 1.2 inch. The 1.2 inch deflection of the cylinder is greater than the maximum response obtained in this experiment. A shunt resistor (249 k ohm) was placed in the amplifier circuit in order to periodically check the amplifier gain in order to maintain the proper sensitivity. The 249 k ohm shunt resistor in the cylinder response measuring circuit was found to cause a -0.32 volt output.

Two force transducers were used to measure the time history of the fluid lift forces (F_L). Force transducer

No. 1 (Sensotec Model LKAF-30, capacity: 10 lb) which is placed just above the cylindrical model measures the resultant force (combined fluid lift and cylinder inertia forces) acting on a cylinder. Force transducer No. 2 (Sensotec Model LKSA-30, capacity: 50 gr) measures only an inertia force of a small mass which is attached to this force transducer and is subjected to the same acceleration as the cylindrical model. Then, assuming the fluid forces in air to be essentially zero, the inertia effect of the cylinder can be eliminated from the force transducer No. 1 signal by adjusting the amplifier gain for the force transducer No. 2 until the sum of the outputs from the two transducers becomes zero when the cylinder oscillates in air. When the inertia force was eliminated as much as possible, the 249 k ohm shunt resistor was found to cause a 0.54 volt output for the 1 inch OD cylinder and a 0.72 volt output for the 2 inch OD cylinder in the output of the force transducer No. 2. This fact was used to periodically adjust the amplifier gain to maintain the proper sensitivity.

The linearity and scale factor of the force transducer No. 1 and the amplifier circuit were obtained by attaching a horizontal string to the cylinder with the water removed. The string passed over a smooth pully and was attached to a small pan. Gram weights were placed on

the pan and the output voltage was recorded from a digital volt meter. A typical statistical analysis of the calibration data gave a straight line calibration curve with a slope (or sensitivity) of 2.08 volt/lb (= 0.468 volt/N), a correlation coefficient of 0.9999, and a standard estimate of error of $\pm$ 6.39 x 10^{-3} lb. ($\pm$ 2.84 x 10^{-2} N). The force range is in the order of $\pm$ 4.0 lb. ($\pm$ 17.8 N). The 249 k ohm shunt resistor in the force transducer No. 1 circuit was found to cause a 4.52 volt output.

Then the cross sensitivity of this force measuring system was checked using static forces. The force transducer No. 1 output was recorded while known static forces acting in the perpendicular direction were applied. For example, while giving a known static force in the x-direction the force transducer No. 1 output in the y-direction was measured. In this experimental set-up, the cross sensitivity was found to be 0.104 volt/lb (2.35 x 10^{-2} volt/N). Less than 5 per cent cross sensitivity was noticed in this force measuring system.

C. Experiments

In this experiment, the cylinder driving method was chosen to give relative motion between fluid and cylinder. As shown in Figure 4, a cylindrical model is mounted on

flexures just below Plate C which was driven with sinusoidal translatory motion of $x = A \sin \omega_d t$ in the input direction (x-direction) where x is the displacement, A is the amplitude of driving motion, ω_d is the angular frequency of driving motion and t is time. Both Plate C and the cylinder model can either respond or be constrained by constraint cables when in place in the output direction (y-direction) as shown in Figure 4. Plate C was mounted on Plate B by aluminum flexures in order to provide the y-direction flexibility.

Two different sizes of thin-walled light aluminum circular cylinders were used as test specimens. The detailed specifications of each cylinder are:

1) D = 1.0 inch
   length: 29.2 inch
   weight: 432 gram (includes fixture)
   wall thickness: 0.065 inch

2) D = 2.0 inch
   length: 28.5 inch
   weight: 629 gram (includes fixture)
   wall thickness: 0.065 inch

To systematically accumulate data, the cylinder input frequency (f_d) was varied from 0.067 Hz to 0.67 Hz and the cylinder input amplitude (A) was also varied from 3 inch to 19 inch. For each cylinder input frequency (f_d) and input amplitude (A), the fluid lift forces (F_L) and the y-direction cylinder responses were monitored using a Norland model 3001 programmable digital oscilloscope.

These signals were analyzed using the Norland to obtain the frequency components of interest, root mean square (R.M.S.) values of the fluid lift force and the cylinder responses...etc., as shown in Figure 3. The detail method to obtain all the frequency components of interest and all the useful R.M.S. values are given below.

1) f_{ns} (Standard natural frequency of a cylinder in y-direction)

The natural frequency of the cylinder in y-direction was obtained by taking the y-direction free damped oscillation signal of the cylinder in still water. It was found that the natural frequency is dependent on the amplitude of the cylinder response in y-direction. For convenience, the standard natural frequency (f_{ns}) was defined as the natural frequency when the cylinder R.M.S. response to cylinder diameter ratio (Y_{RMS}/D) is around 0.1.

The standard natural frequency, when the cylinder length submerged in water (ℓ) is 22 inch, is 1.585 Hz for the 1 inch diameter cylinder and 1.445 Hz for the 2 inch diameter cylinder.

2) f_v (Vortex shedding frequency)

The vortex shedding frequency (f_v) was obtained by taking the power spectral density of the measured fluid lift force signal using the Norland. Among the several

peaks in the power spectral density, the highest peak was considered to correspond to the vortex shedding frequency (f_v).

3) f_d (cylinder input frequency)

The cylinder input frequency (f_d) was constantly monitored during the experiment using the on-off signal from the microswitch placed at one end of the cylinder oscillating amplitude. Then the on-off signal was transmitted to the Hewlett Packard model HP 528 D frequency counter. It was found that the input frequency (f_d) could be maintained constant within 0.5 per cent error during the experiment.

4) f_r (Cylinder response frequency)

The cylinder response frequency (f_r) was obtained by taking the power spectral density of the measured cylinder response signal using the Norland. The highest peak of the power spectral density was chosen as the cylinder response frequency (f_r).

5) f_n (Cylinder natural frequency in y-direction)

During the experiment, it was observed that the cylinder natural frequency in y-direction varies with both the cylinder input frequency (f_d) and amplitude (A).

The cylinder natural frequency in y-direction was obtained by examining the power spectral density of the cylinder response signal in the Norland. It was found that the cylinder responds in y-direction with its natural frequency. In other words, the cylinder response frequency (f_r) is equal to the cylinder natural frequency (f_n) in almost all of the cases. However, when the locked-on condition occurs, it was found that the cylinder response frequency (f_r) differed from the natural frequency (f_n). so that the closed Lissajous loop as shown in Figure 1 was obtained. Both the cylinder's natural and response frequencies could be easily detected from the power spectral density of the cylinder response signal in the y-direction when the locked-on condition occurred.

Besides all of the above frequencies of interest, the R.M.S. values of the cylinder response and fluid lift force signal and the peak values of the fluid lift force were automatically obtained using programs in the Norland model 3001 data analyzing unit. The programs used in the Norland are listed in Appendix C.

Keulegan and Carpenter [7] and Sarpkaya [9] made a simple dimensional analysis for the case of uniform harmonic fluid motion around a fixed circular cylinder and suggested that the force coefficients can be written as

$$\text{Force coefficients} = f\left(\frac{U_m T}{D}, \frac{U_m D}{\nu}\right). \qquad (2)$$

$$= f(\text{Keulegan-Carpenter number, Reynolds number})$$

where

U_m: Maximum fluid velocity (Maximum cylinder input velocity) ($= A\omega_d$)

T: Period of harmonic fluid motion (Period of cylinder input motion)

D: Cylinder diameter

ν: Kinematic viscosity of fluid.

Evidently, $U_m T/D$ may be replaced by $2\pi A/D$ or simply A/D.

where

A: Amplitude of harmonic fluid motion (Amplitude of cylinder input motin)

This study deals with the periodic fluid flow around an elastically mounted cylinder as well as around a fixed cylinder. Since the self-induced cylinder response in y-direction can significantly affect the force coefficients, it is natural to add several more parameters besides Reynolds and Keulegan-Carpenter numbers for the case of an elastically mounted cylinder. Four more nondimensional numbers are used in this work and are described as follows.

$$S_t = \frac{f_v D}{U_m} = \frac{1}{2\pi}\frac{D}{A}\frac{f_v}{f_d} \quad \text{(Strouhal number for periodic flow)} \qquad (3)$$

$$V_R = \frac{Af_d}{Df_r} = \frac{A}{D}\frac{\omega_d}{\omega_r} \qquad \text{(Velocity ratio)} \qquad (4)$$

$$V_R^* = \frac{Af_d}{Df_{ns}} = \frac{A}{D}\frac{\omega_d}{\omega_{ns}} \qquad \text{(Velocity ratio using } f_{ns}\text{)} \qquad (5)$$

$$FR = \frac{f_{ns}}{f_d} \qquad \text{(Frequency ratio)} \qquad (6)$$

where

f_v: Vortex shedding frequency $(= \frac{\omega_v}{2\pi})$

f_d: Frequency of periodic fluid flow (Cylinder input frequency) $(\frac{\omega_d}{2\pi})$

f_r: Cylinder response frequency $(= \frac{\omega_r}{2\pi})$

f_{ns}: Standard cylinder natural frequency $(= \frac{\omega_{ns}}{2\pi})$

All the above nondimensional numbers were found to be effective in explaining the experimental data.

IV. EXPERIMENTAL DATA ANALYSIS

A. A Lift Force Model

As the cylinder is driven back and forth in a fluid at rest as shown in Figure 4, vortex shedding occurs and periodic lift forces begin to act on the cylinder. The cylinder, in turn, begins to respond in the y-direction. Like the wake oscillator model for uniform fluid flow around an elastic cylinder, this cylinder motion can be considered as a single degree of freedom forced damped vibration. For this case, the governing differential equation for cylinder motion can be written as

$$M_s\ddot{y} + C_{sy}\dot{y} + k_y y = F_L^*(x, \dot{x}, y, \dot{y}, \ddot{y}, \rho, \mu, D, \ell) \qquad (7)$$

where

M_s: structural mass

C_{sy}: structural damping coefficient in y-direction

k_y: structural stiffness in y-direction

ρ: fluid density

μ: fluid viscosity

D: cylinder diameter

ℓ: cylinder length submerged in fluid

x: cylinder driving (input) displacement

$\dot{x}$: cylinder driving (input) velocity

y: cylinder response (output) displacement

$\dot{y}$: cylinder response (output) velocity

$\ddot{y}$: cylinder response (output) acceleration

After considering that the lift forces are due to periodic vortices, a simple fluid lift force model is proposed to be given by

$$F_L^*(t) = C_L \frac{\rho U_x^2 D \ell}{2} \text{ Sin } (\omega_v t) - C_f \dot{y} - C_{my} \frac{\pi D^2 \rho \ell}{4} \ddot{y} \qquad (8)$$

where

C_L: lift force coefficient

U_x: cylinder driving (input) velocity

ω_v: vortex shedding angular frequency

C_f: fluid damping coefficient

C_{my}: fluid added mass coefficient in the y-direction

Since the cylinder is driven sinusoidally, the cylinder velocity becomes

$$U_x = A\omega_d \text{Sin}(\omega_d t) \qquad (9)$$

where

ω_d: cylinder driving (input) angular frequency

From Equations 7, 8 and 9, there results

$$M\ddot{y} + C\dot{y} + k_y y = C_L \frac{\rho D \ell}{2} (U_x)^2 \sin(\omega_v t) \qquad (10)$$

where

$M = M_s + C_{my}(\frac{\pi D^2 \rho \ell}{4})$: Total system mass

$C = C_s + C_f$: Total damping coefficient

then,

$$F_L^*(t) = C_L \frac{\rho D \ell}{2} (U_x)^2 \sin(\omega_v t)$$

$$= C_L \frac{\rho D \ell}{2} (A\omega_d)^2 \sin^2(\omega_d t) \sin(\omega_v t) \qquad (11)$$

From Equation 11 it can be seen that the vortex shedding frequency and the cylinder driving frequency play an important role in determining the fluid lift forces.

The vortex shedding frequency was observed to be related to the A/D ratio and the cylinder driving frequency (f_d). Except for several special cases (when f_n/f_d = integer... etc.), the resulting vortex shedding frequency made the Strouhal number ($S_t = \frac{f_v D}{U_m} = \frac{1}{2\pi} \frac{f_v D}{f_d A}$) drop into the range of 0.15 - 0.20.

It is worthwhile to consider the ratio of vortex shedding frequency to the cylinder driving frequency. For this purpose let

$$\frac{f_v}{f_d} = \frac{\omega_v}{\omega_d} = n \qquad (12)$$

where the physical meaning of this ratio is the number of vortices generated during one back and forth oscillation of the cylinder; i.e., vortices/cylinder input (driving) cycle.

From Equations 11 and 12

$$F_L^*(t) = C_L \frac{\rho D \ell}{2} (A\omega_d)^2 \sin^2(\omega_d t) \sin(n\omega_d t)$$

$$= C_L \frac{\rho D \ell}{2} (A\omega_d)^2 \frac{1-\cos(2\omega_d t)}{2} \sin(n\omega_d t)$$

$$= C_L \frac{\rho D \ell}{4} (A\omega_d)^2 \left[\sin(n\omega_d t) - \frac{1}{2}\sin(n+2)\omega_d t - \frac{1}{2}\sin(n-2)\omega_d t \right]$$

Then the lift force becomes

$$F_L^*(t) = C_L \frac{\rho D \ell}{8} (A\omega_d)^2 \left[2\sin(n\omega_d t) - \sin(n+2)\omega_d t - \sin(n-2)\omega_d t \right] \tag{13}$$

Judging from Equation 13, the expected frequency components of fluid lift forces are nf_d, $(n+2)f_d$ and $(n-2)f_d$; or f_v, $f_v + 2f_d$ and $f_v - 2f_d$ where $f_d = \frac{\omega_d}{2\pi}$. According to this model in Equation 13, the largest frequency component is the one corresponding to the vortex shedding frequency with two small side band components. The amplitude of these three components is dependent on the cylinder driving frequency (f_d) and amplitude of input motion (A).

As mentioned previously, the f_v/f_d ratio is determined by the A/D ratio and the Strouhal number (S_t). To verify this fluid lift model, a comparison between the theoretical

shape of the lift force and the experimentally measured lift force was made.

A measured fluid lift force time history for A/D = 6.0 (D = 2.0 inch and A = 12.0 inch) and f_d = 0.154 Hz acting on a fixed cylinder (no responses in y-direction) is shown in Figure 5. The corresponding frequency components of the measured lift force are shown in Figure 6. Figure 6 was obtained by taking power spectral density of the measured fluid lift force signal. Here it is evident that there are three significant frequency components. The largest of these components occurs at a frequency that is 7 times the cylinder driving frequency (f_d). That means $f_v/f_d = 7$ and indicates that 7 vortices are generated during one back and forth cylinder input oscillation. And also the two side bands occur at $5f_d$ (which is $f_v - 2f_d$) and $9f_d$ (which is $f_v + 2f_d$) as predicted from the simple theoretical model of Equation 13. The theoretical shape of the fluid lift force time history was drawn from equation 13 using n = 7 and is also shown in Figure 5 where A, B, and C are used to identify equivalent peaks. The general agreement in wave shape between the measured and predicted time history is remarkable considering the complexity of the phenomenon where the cylinder moves back and forth in its own wake.

During the experiment, it was noticed that the shape of the lift forces was not always consistent; i.e., the f_v/f_d ratio changed from time to time. The f_v/f_d ratio was found to vary with little or no change in the cylinder driving (input) conditions. These variations in behavior are most likely due to the complex mechanisms associated with the vortex shedding characteristics of a cylinder moving in its own wake. These vortex shedding changes are related to the Strouhal number (S_t) and the f_v/f_d ratio as discussed in the following sections.

B. The Natural Frequency of the Cylinder in Y-direction (f_n)

The natural frequency of the elastically mounted cylinder was found to vary with operating conditions, suggesting that the problem is nonlinear as most fluid-structure interaction problems are.

If it is assumed that the damping is very small, the natural frequency of a cylinder in y-direction is obtained from Equation 10 to be

$$f_n = \frac{1}{2\pi}\sqrt{\frac{k_y}{M}} \tag{14}$$

In the calibration procedure, it was observed that the stiffness in y-direction (k_y) is constant for deflections less than 1.2 inches. This implies that the natural

frequency variation is due to a change in the fluid added mass.

It was observed that the change in natural frequency can be related to several parameters such as the cylinder response in the y-direction (y), the ratio of cylinder driving motion amplitude to cylinder diameter ratio (A/D), and the cylinder driving frequency (f_d).

First, the effect of cylinder response motion (y) on the cylinder natural frequency was examined. For a 2 inch diameter cylinder, a damped free oscillation signal in still water was monitored. From this y-direction damped free oscillation signal, the variation of the natural frequency with cylinder response was observed. For convenience, two nondimensional numbers were introduced. The first is the ratio of natural frequency to the already defined standard natural frequency (f_n/f_{ns}) and the second is the ratio of R.M.S. response of the cylinder to cylinder diameter (y_{RMS}/D). Assuming that each cycle of the damped free oscillation is sinusoidal, the R.M.S. value of the cylinder response (y_{RMS}) could be calculated by multiplying the peak cylinder response by 0.707.

Then, the natural frequency ratio (f_n/f_{ns}) for a 2 inch diameter cylinder was plotted against the ratio of R.M.S. cylinder response to cylinder diameter (y_{RMS}/D)

as shown in Figure 7. It can be seen in Figure 7 that the variation of cylinder natural frequency due to the cylinder responses is less than 1 per cent so long as y_{RMS}/D is less than 0.4. It is known that the maximum response of an elastically mounted cylinder exposed to uniform fluid flow is about one diameter peak to peak. That is equivalent to a y_{RMS}/D ratio of 0.35. Considering the uniform fluid flow around an elastically mounted cylinder, 0.4 was chosen as the estimated maximum y_{RMS}/D ratio in case of an oscillating flow around an elastically mounted cylinder. A value of 0.4 was obtained by experiment. Figure 7 also shows the natural frequency decreases as the cylinder responses increase. This trend suggests that the fluid added mass increases as the cylinder responses grow.

Next, the A/D ratio and the cylinder driving frequency (f_d) effect on the natural frequency was carefully examined. As discussed previously, the cylinder natural frequency in the y-direction was obtained by taking the power spectral density of the cylinder response signal while varying the cylinder driving conditions (cylinder driving amplitude to diameter ratio (A/D) and the cylinder oscillating frequency (f_d)). Special care was taken to choose natural frequency from the power spectral density of the cylinder response signal as explained before. Then the natural frequency ratio

(f_n/f_{ns}) for a 2-inch diameter cylinder was plotted against the nondimensional number $V_R^*(=\frac{Af_d}{Df_{ns}})$ as shown in Figure 8. The least squares statistical analysis of the plot in Figure 8 shows that the natural frequency ratio is constant when $V_R^* < 0.95$ and the ratio varies linearly with V_R^* when $V_R^* > 0.95$.

For the 2-inch diameter cylinder

$$\frac{f_n}{f_{ns}} = 1.0 \qquad \text{when } V_R^* < 0.95 \tag{15}$$

$$\frac{f_n}{f_{ns}} = 0.17\ V_R^* + 0.84 \quad \text{when } V_R^* > 0.95 \tag{16}$$

The correlation coefficient for the straight line fit of these data points is 0.93. As shown in Figure 8 the natural frequency is seen to be constant when $V_R^* < 0.95$ (for relatively slow cylinder driving frequency along with large motion in the y-direction) and to increase linearly when $V_R^* > 0.95$ (for relatively fast driving frequency along with small motion in the y-direction). It was observed that the natural frequency increases about 10 per cent above the standard natural frequency (f_{ns}) when V_R^* reaches 1.50. This means that the effective mass of the cylinder appears to decrease as V_R^* increases implying that the fluid added mass must decrease with an increasing V_R^*. The frequency ratio (f_n/f_{ns}) for the 2-inch diameter cylinder when driving

in air was measured to be 1.11 (f_n = 1.601 Hz and f_{ns} = 1.445 Hz). Hence, it is anticipated that the cylinder has negative added mass when V_R^* exceeds 1.56 as shown in Figure 8. These results are similar to those obtained by Sarpkaya [9]. He measured negative added mass from oscillating fluid flow around a fixed cylinder. It is not known whether Equations 15 and 16 apply to other sized cylinders since different sized cylinders have different fluid added mass. It is believed, however, that the trends for variation of cylinder natural frequency are the same for other sized cylinders. The cylinder added mass due to fluid flow around the cylinder increases as the cylinder response increases. On the other hand, the fluid added mass decreases as the nondimensional number V_R^* increases above a value around unity.

At this point, it is only an interesting observation to note that V_R^* is the ratio between the maximum input velocity (cylinder driving velocity) $U_x = 2\pi f_d A$ and the maximum response velocity in the y-direction at reasonance $U_y = 2\pi f_{ns} D$ assuming the maximum response is about one diameter.

C. The Vortex Shedding Frequency (f_v)

The vortex shedding frequency (f_v) plays a very important role in determining the cylinder response and

the fluid lift forces acting on the cylinder. Judging from Equation 10, the vortex shedding frequency (f_v) determines the shape of the exciting forces acting on a cylinder in y-direction. It can be anticipated that when the vortex shedding frequency matches with the system natural frequency, a resonance condition takes place.

The so-called Strouhal number (S_t) is widely used to describe the vortex shedding phenomenon whether the fluid flow around a cylinder is steady or unsteady. In the 19th century, Strouhal was the first to relate the vortex shedding frequency to the fluid flow velocity and the cylinder diameter and defined the Strouhal number (S_t) for steady fluid flow around a circular cylinder. It is not proper to use the Strouhal number, defined for steady flow, in unsteady fluid flow problems since the fluid flow velocity is not constant. However, with some modification, the Strouhal number (S_t) can be used for certain unsteady flow problems. Sarpkaya [9] used Strouhal number for oscillating fluid flow by replacing the steady fluid flow velocity with the maximum fluid flow velocity. For a circular cylinder the Strouhal number (S_t) is usually defined as

$$S_t = \frac{f_v D}{U} \qquad \text{for steady flow} \qquad (17)$$

which is modified to

$$S_t = \frac{f_v D}{U_m} \qquad \text{for periodic flow} \qquad (18)$$

where

D: cylinder diameter

U: fluid velocity in steady flow

U_m: Maximum fluid velocity in oscillating flow ($= A\omega_d$)

It is well-known that the Strouhal number (S_t) is approximately 0.2 for a fixed smooth cylinder located in steady uniform fluid flow in the subcritical Reynolds number range of 500 to 100,000 [3, 41]. In the oscillating fluid flow case, vortex shedding behavior is not as simple as it is in the steady fluid flow case since the cylinder moves in its own wake. Sarpkaya [8, 9] studied Strouhal number variations for a fixed cylinder located in an oscillating fluid flow. He concluded that S_t does not remain constant around 0.2 in the subcritical Reynolds number region as in the steady flow case. He also found that S_t depends on both K (Keulegan - Carpenter number or period parameter) and Re (Reynolds number). Sarpkaya observed the upper limit of the S_t to be about 0.2 for Reynolds numbers smaller than about 50,000. At large values of Re, the S_t increases to about 0.3 in oscillating fluid

flow around a fixed cylinder. On the other hand, Griffin [21] studied the vortex shedding frequency in the wake of an oscillating cylinder. He observed the S_t variations for a cylinder oscillating normal to a uniform steady fluid flow. He found the wake S_t to be 0.178 for Reynolds number in the range of 700 to 50,000.

This research deals with the behavior of a cylinder free to respond to an oscillating fluid flow and is equivalent to a combination of both Sarpkaya's and Griffin's experimental conditions.

In this experiment, the vortex shedding frequency (f_v) was obtained from the power spectral density frequency measurements of the directly measured fluid lift forces acting on a cylinder. Out of several peaks from the fluid lift force power spectral density, the largest peak was considered to be the vortex shedding frequency as predicted from the Equation 13.

All the experiments were performed in the range of Re = 3,000 to 40,000 and $K(=2\pi\frac{A}{D})$ = 15 to 120. In order to portray the relationship between vortex shedding frequency f_v, the cylinder driving frequency f_d, the Keulegen - Carpenter number K, and Strouhal number S_t, the f_v/f_d ratio was plotted as a function of K as shown in Figure 9 for several different cylinder driving frequencies. The cylinder was both fixed and released

for these measurements. A released cylinder means that the cylinder oscillates with free responses in the y-direction, while a fixed cylinder is the case where the cylinder is constrained from moving in the y-direction.

As shown in Equation 18, the Strouhal number in an oscillating fluid flow can be determined if the f_v/f_d ratio and the Keulegan - Carpenter number are known since $f_v/f_d = S_t \times K$. Thus a constant Strouhal number gives a straight line in Figure 9. For reference, two constant Strouhal number lines of $S_t = 0.15$ and $S_t = 0.20$ were drawn in Figure 9. In the case of the fixed cylinder exposed to oscillating fluid flow, the Strouhal number always drops in the narrow range of from 0.15 to 0.20 for all the different cylinder driving frequencies and different Keulegan - Carpenter numbers. This fact matches quite well with Sarpkaya's results [9]. He found that the Strouhal number is not constant for oscillating fluid flow around a fixed cylinder as is the case for steady fluid flow. He found that S_t varies for periodic fluid flow with S_t having an upper limit of 0.20 in the sub-critical range of Reynolds number. In the released cylinder case, it was found that the Strouhal number is also in the 0.15 to 0.20 range with one exception. That exception is the so-called locked-on region. In addition

to the locked-on phenomenon, several other important facts should be noted in regard to Figure 9.

First, the vortex shedding frequency (f_v) increases with increasing values of the Keulegan - Carpenter number (K) for both the fixed and released cylinder. Many previous studies have been done on the vortex shedding frequency (f_v). Those by Bidde [38], Sarpkaya [9], and Isaacson [42] are particularly important to note here. Bidde [38] and Sarpkaya [9] said that the vortex shedding frequency (f_v) increases as K increases and also found $f_v = 2f_d$ independent of the value of the Keulegan - Carpenter number. On the other hand, Isaacson [42] could not find the vortex shedding frequency at twice the cylinder oscillating frequency ($f_v = 2f_d$). He only found that the vortex shedding frequency (f_v) increases with K; a result that supports the results shown in Figure 9.

Second, for low Keulegan - Carpenter numbers, the f_v/f_d ratio always had an integer value. On the other hand, for relatively high K (for $K > 80$) noninteger f_v/f_d ratios were observed. As mentioned before, the f_v/f_d ratio is a measure of the number of vortices actually shed during a single back and forth cylinder motion. For relatively low values of K and A/D ratio, the number of vortices generated during a single cylinder driving period occur as integer multiples of the cylinder driving

frequency f_d. Apparently, under these integer conditions, it is possible to have the vortices take up fixed relative positions with respect to one another so that the cylinder moves easily amongst the vortices as shown in Figure 4. Each cylinder/vortex interaction causes two things to happen. First, a locked-on vortex strengthening takes place so that the correlation of vortex shedding along the length of the cylinder is improved. Second, the improved correlation causes larger lift forces so that the cylinder responds with larger amplitudes in the y-direction. Also it must be pointed out that under these conditions, the cylinder returns to a previously shed vortex before that vortex has any significant time to escape from its location relative to the cylinder motion. The above entrapment of vortices in a fixed spatial pattern begins to break down when the Keulegan - Carpenter number exceeds a value of approximately 80 ($A/D > 13$). In this case, a large number of vortices are generated for each back and forth cylinder motion. There is sufficient time for a vortex generated during the initial part of the cylinder driving motion to dissipate as well as change location before the cylinder returns to interact with that vortex a second time. This type of fluid structure interaction causes inconsistent vortex shedding as well as noninteger f_v/f_d ratios as shown in Figure 9.

Third, the most important factor to be locked-on is that fn/fd = fv/fd = integer. More details about the locked-on phenomenon will be discussed in a latter section.

D. The Cylinder Response Frequency (f_r)

The cylinder response frequency (f_r) was obtained from the power spectral density frequency analysis of the cylinder response signal. Then the nondimensional number $\frac{1}{2\pi V_R}$ ($=\frac{Df_r}{2\pi Af_d}$) is plotted against the f_{ns}/f_d ratio in Figure 10 for the 1 inch cylinder and in Figure 11 for the 2 inch cylinder. In these figures, the straight lines with different A/D ratios show the case where the cylinder vibrates in the y-direction with the cylinder standard natural frequency, f_{ns} (D = 1.0; f_{ns} = 1.585 Hz, D = 2.0; f_{ns} = 1.445 Hz when ℓ = 22 inch). In other words, the straight lines show the case when $f_r = f_{ns}$. It can also be seen in those figures that most of the points lie on the straight line with two exceptions. The first is the locked-on region while the second is the lower part of each line, especially for the 2-inch cylinder. As discussed before, the differences between the straight line and the data points in the lower part of each line is due to the cylinder natural frequency variation. Already it was mentioned that the cylinder natural frequency (f_n) for the 2-inch cylinder increases up to more than 10

per cent above the standard natural frequency (f_{ns}) as V_R increases as shown in Figure 8.

A strong tendency to be locked-on was observed during the experiments when an integer f_{ns}/f_d ratio occurred; especially when the A/D ratio is less than 10 and the value of $1/(2\pi V_R)$ is in the range of from 0.15 to 0.32.

Usually the locked-on phenomenon is explained as the fact that the vortex shedding frequency (f_v) adheres to the cylinder natural frequency (f_n) when a bluff body is exposed to a steady fluid flow and subjected to vortex induced vibration in the wake.

In the case of an oscillating fluid flow around a circular cylinder as in this experiment, another type of locked-on phenomenon was observed. The vortex shedding frequency (f_v) changes to match either the cylinder natural frequency (f_n) or to the cylinder response frequency (f_r). That is, the cylinder response frequency (f_r) tracks the vortex shedding frequency so that the f_r/f_d ratio remains an integer in the region of an integer f_n/f_d ratio. In other words, the cylinder response is determined to make the cylinder follow a path in the fluid so that a closed loop is formed when the f_n/f_d ratio is in the region of an integer value. The steps in the straight lines shown in Figure 10 and Figure 11 indicate when locked-on and a closed cylinder path occur. It is natural to say that a

lower A/D ratio can give the locked-on condition more easily than a higher A/D ratio case. For the low A/D ratio case, the vortex shedding pattern is more consistent than in the high A/D ratio case as discussed previously. Thus it is harder to be locked-on for large A/D ratios, since the vortex shedding is inconsistent compared to the low A/D ratio case.

It seems that the locked-on phenomenon is a combined result of the vortex shedding frequency (f_v), the cylinder natural frequency (f_n), the cylinder driving frequency (f_d), the cylinder response frequency (f_r), and the driving amplitude to cylinder diameter ratio (A/D).

Before running the experiment, it was suspected that the f_n/f_d ratio is the most important factor to the locked-on phenomenon. As shown in Figure 10 and Figure 11 all the locked-on phenomenon were observed near integer f_n/f_d ratio. A low A/D ratio has a wider range of f_{ns}/f_d for locked-on to occur than in the large A/D ratio case. It was suspected that the A/D ratio played an important role for the locked-on condition to occur, particularly integer values. It was found that integer ratios do not make a big difference. On the other hand, the f_n/f_d ratio having integer values is very important in determining the cylinder locked-on condition.

The cylinder natural frequency (f_n) was also obtained from the power spectral density frequency analysis of the

cylinder response signal in exactly the same way as the cylinder response frequency (f_r). The cylinder response frequency (f_r) could be identified from the cylinder natural frequency (f_n) by considering the locked-on phenomenon around an integer f_n/f_d ratio. Except for the locked-on regions, the cylinder response in the y-direction was at its natural frequency (f_n). Only in the locked-on region was the cylinder response frequency (f_r) different from its natural frequency (f_n).

E. The Relationship between the Vortex Shedding Frequency (f_v), the Cylinder Natural Frequency (f_n), and the Cylinder Response Frequency (f_r)

If the cylinder driving frequency (f_d) and the A/D ratio are known, then the vortex shedding frequency (f_v) determines the corresponding Strouhal number ($S_t = Df_v/(2\pi Af_d)$), the cylinder response frequency (f_r) determines V_R ($= (Af_d)/(Df_r)$) and the standard natural frequency (f_{ns}) determines $V_R^*(= (Af_d)/(Df_{ns}))$. In order to directly compare all three frequency components (f_v, f_n, and f_r), $1/(2\pi)$ was multiplied to the inverse of V_R and V_R^*. These three quantities (S_t, $1/(2\pi V_R)$, and $1/(2\pi V_R^*)$) were plotted together against the f_{ns}/f_d ratio in the upper part of Figures 12 through 16 for different A/D ratio and cylinder diameters. In those figures, the

solid straight line represents the $1/(2\pi V_R^*)$ (= $(Df_{ns})/(2Af_d)$) numbers, the 'Δ' character is for the Strouhal number S_t (= $(Df_v)/(2\pi Af_d)$), and the 'o' character is for the non-dimensional number $1/(2\pi V_R)$ (= $(Df_r)/(2\pi Af_d)$). A careful examination of these figures reveals that the graphs can be divided into three distinct regions; lower, mid, and upper parts of the f_{ns}/f_d ratio.

In the lower f_{ns}/f_d ratio region, the vortex shedding frequency (f_v) is always higher than the cylinder response frequency (f_r) and the cylinder natural frequency (f_n). In this region, a very interesting relationship between the vortex shedding frequency (f_v) and the cylinder response frequency (f_r) was observed to be $f_r = f_v - 2f_d$. This means that the cylinder response frequency (f_r) is the same with the lower side band of the lift force model given in Equation 13. In other words, the cylinder exciting frequency (the vortex shedding frequency) mismatches with the cylinder response frequency by two times the cylinder dividing frequency in this region.

Figure 17 shows a typical frequency analysis for this lower f_{ns}/f_d ratio region. The case shown (A/D = 6.0 and f_{ns}/f_d = 5.30) matches with the lower f_{ns}/f_d ratio section of Figure 16. These peaks (1.514 Hz, 2.100 Hz, and 2.660 Hz) were found in this lift force frequency analysis as expected from the lift force model, Equation 13. In addition, it

was observed that the cylinder response frequency (f_r) occurs at 1.514 Hz (= 5.30 f_d) and mismatches with the main vortex shedding frequency (f_v) of 2.100 Hz (7.35 f_d) by 2 f_d. In other words, the lower side band of the lift force excites the cylinder in the lower f_{ns}/f_d ratio region.

For the mid-range of the f_{ns}/f_d ratio, the vortex shedding frequency (f_v) always matches with the cylinder response frequency (f_r) and the cylinder natural frequency (f_n). It was also observed that the vortex shedding frequency (f_v) changes to make the Strouthal number stay in the range of from 0.15 to 0.20.

Figure 18 shows a typical frequency analysis for a mid-range of the f_{ns}/f_d ratio. The case shown (A/D = 6.0 and f_{ns}/f_d = 6.22) matches with the mid-range of the f_{ns}/f_d ratio of Figure 16. Three peaks (0.990 Hz, 1.464 Hz, and 1.953 Hz) were also found in the lift force frequency analysis, similar to the lower f_{ns}/f_d ratio region case. It was found that the cylinder response frequency (f_r) occurs at 1.464 Hz (= 6.22 f_d) and matches the main vortex shedding frequency (f_v) which occurs also at 1.464 Hz (= 6.22 f_d). In this case, the vortex shedding frequency (f_v) excites the cylinder at its natural frequency. The resulting cylinder motion and the vortex sheddings strongly interact and support each other to give large amplitudes

of cylinder responses. The so-called locked-on phenomenon appears in this mid-range of the f_{ns}/f_d ratio.

For the upper range of the f_{ns}/f_d ratio, the vortex shedding frequency (f_v) is always lower than the cylinder response frequency (f_r) except for several data points which correspond to a locked-on condition. In most of the cases of this upper region, the vortex shedding frequency adjusts to make the Strouhal number between 0.15-0.20. This result is the same as that obtained for a fixed cylinder exposed to an oscillating fluid flow as discussed previously. The reason why the Strouhal number in the upper region of the f_{ns}/f_d ratio appear similar to those for the fixed cylinder case is that there occurs little cylinder response, giving a nearly constrained condition.

Figure 19 shows a typical frequency analysis for the upper region of the f_{ns}/f_d ratio. The case shown (A/D = 6.0 and f_{ns}/f_d = 8.89) corresponds to the upper f_{ns}/f_d ratio region in Figure 16. In this case, the cylinder is excited by three lift force components locked at 0.732 Hz (= 4.94 f_d), 1.02 Hz (= 6.92 f_d) and 1.318 Hz (= 8.89 f_d). The dominant lift force component occurs at 1.025 Hz (= 6.92 f_d), suggesting this to be the vortex shedding frequency with two side band components of 4.94 f_d and 8.89 f_d as predicted in Equation 15. The dominant cylinder response frequency (f_r), however, occurs at 1.318 Hz (= 8.89 f_d),

(giving the relationship of $f_r = f_v + 2f_d$. In other words, the cylinder is excited by the upper side band component of the lift forces. The cylinder response frequency (f_r) mismatches with the vortex shedding frequency by two times the cylinder oscillating frequency (f_d). However, Figures 12 to 16 show that the $f_r = f_v + 2f_d$ relationship in the upper f_{ns}/f_d region is not as consistent as in the lower f_{ns}/f_d ratio region where $f_r = f_v - 2f_d$ was consistently maintained. A clear reason could not be found in this work. It is believed, for the upper f_{ns}/f_d ratio region, that the strength of vortex shedding seems to be less strong than in the mid and lower f_{ns}/f_d ratio regions. In turn, this causes weaker cylinder responses so that the cylinder response frequency (f_r) becomes less correlated with the vortex shedding frequency (f_v).

F. The Cylinder Response Amplitude in Y-direction (y)

In this section, the cylinder response in the y-direction due to an oscillating fluid flow was closely examined. The R.M.S. (root mean square) value of cylinder response (y_{RMS}) was calculated to represent the cylinder response amplitude and the y_{RMS}/D ratio was plotted against the f_{ns}/f_d ratio in the lower part of Figures 12 to 16 for different diameters and A/D ratios. The f_{ns}/f_d ratio

was chosen for the independent variable because it is believed to be the most important parameter for determining the cylinder responses. By combining these data with the frequency analysis results on the same graph sheet, it is easy to directly compare results as shown in Figures 12 to 16.

Several (Griffin [21]; Durgin, March, and Lefebvre [43]; ...etc.) investigators have studied self-excited cylinder oscillations placed in a uniform steady flow. Griffin [21] observed and studied the self-limiting cylinder motion for an elastically mounted cylinder in uniform fluid flow. He found that as the amplitude of cylinder vibration is increased beyond approximately 0.5D, the symmetric pattern of alternately spaced vortices began to break up. He concluded that this vortex break up implies that the vortex induced forces on a cylinder are self-limiting at circular vibration amplitudes on the order of one diameter peak to peak.

In the case of periodic fluid flow, the vortex shedding patterns are much more complicated than for the uniform steady flow case. The one diameter peak to peak maximum response is nearly applicable to the oscillating fluid flow case. It was found that the maximum cylinder response amplitude goes up to 1.15 D peak to peak; and then, tends to decrease as the A/D ratio increases as shown in Figures 12 to 16.

In the periodic fluid flow case, the amplitude of a cylinder response seems to be determined by several factors such as the A/D ratio and all the frequency components which include f_v, f_r, f_n, and f_d. It was observed that certain special cases of these factors strongly affect the cylinder response amplitudes. These special cases are explained as follows.

i) The vortex shedding strength is one of the most important factors in determining the cylinder response amplitude. It was observed that strong vortex shedding occurs when the f_v/f_d ratio is an integer and the Strouhal number ($S_t = (Df_v)/(2\pi Af_d)$ is in the narrow range of 0.15-0.20.

ii) The f_n/f_d ratio is believed to play an important role in determining when large cylinder responses occur. An integer f_n/f_d ratio corresponds to larger amplitudes than the case for a noninteger f_n/f_d ratio.

iii) An integer f_r/f_d ratio corresponds to a closed loop of the cylinder paths. However, an integer f_r/f_d ratio by itself is not sufficient for large amplitudes to occur. It must be associated with an integer f_n/f_d ratio as well as for the sharp increases in cylinder responses to occur.

iv) When $f_r = f_n$, a resonance condition exists. However, as the cylinder response grows, the vortex shedding patterns and the cylinder natural frequency are changed. These changes lead to the self-limiting of the cylinder responses.

To clarify the effects of the A/D ratio and all the frequency components, including f_v, f_r, f_n, and f_d, on the cylinder response amplitudes, the cylinder responses for each special case were carefully examined taking Figure 16 (A/D = 6.0 and D = 2.0 inch) as an example. All the identifying characters (A, B, C, D,...etc.) for each special case were placed on the matching place in Figure 16.

A) $f_r/f_d = f_n/f_d = f_v/f_d$ = Integer, $0.15<S_t<0.20$.

In this case, the cylinder path makes a closed loop (f_r/f_d = integer) and the cylinder vibrates at its natural frequency ($f_r = f_n$). Also high fluid lift forces can be expected from strong and stable vortex shedding patterns (f_v/f_d = integer and $0.15<S_t<0.20$) since the cylinder tends to move around a stable vortex shedding pattern. The highest cylinder response amplitude is expected for this condition.

B) $f_r/f_d = f_n/f_d = f_v/f_d \neq$ integer, $0.15<S_t<0.20$

In this case, the cylinder responds at its natural frequency ($f_r = f_n$) but the cylinder path does not make a

closed loop. This open loop causes the cylinder to pass through its own wake so that the vortex shedding strength is not as high as in the case A. Also the f_v/f_d ratio is not integer in this case. The cylinder response amplitude is still high but less than that of the case A.

C) $f_r/f_d = f_v/f_d$ = Integer $f_r/f_d \neq f_n/f_d$

In this case, the cylinder motion makes a closed loop as in the case A, but the cylinder vibration frequency differs from its natural frequency and significant response amplitude drops were observed.

D) Integer $f_r/f_d \neq$ Integer f_v/f_d, $f_v \neq f_r \neq f_n$, $0.15 < S_t < 0.20$

In this case, the cylinder motion makes a closed loop as in cases A and C, but all the frequency components are different from each other. Even though strong vortices exist for this case, the cylinder response amplitudes are very low due to mismatches of vortex shedding and the cylinder-natural frequencies.

E) $f_r/f_d = f_n/f_d = f_v/f_d - 2 \neq$ Integer, $0.15 < S_t < 0.20$

In this case, the cylinder path does not make a closed loop, but the cylinder vibrates at its natural frequency. As explained previously, the cylinder is excited by the lower side band of the fluid lift force. It seems that the lower side band correlates well with the cylinder natural frequencies and creates strong vortices which, in turn, creates quite high cylinder responses.

In considering all of the above cases, it appears that a certain combination of all the frequency components is more important for determining cylinder response amplitudes in oscillating fluid flow than the standard non-dimensional numbers such as Reynolds number, Keulegan - Carpenter number ... etc. Also this fact can be applied to explain the fluid force coefficient data which are discussed in the next section.

G. The Fluid Lift Force Coefficient ($C_{L(pk)}$ and $C_{L(RMS)}$)

The fluid lift force coefficient was examined for different cylinder diameters and A/D ratios. From Equations 10 and 11, the peak and R.M.S. fluid lift force coefficient can be defined as

$$C_{L(pk)} = \frac{\text{Max. Lift Force}}{0.5\rho D\ell(A\omega_d)^2} \tag{19}$$

$$C_{L(RMS)} = \frac{\text{R.M.S. of Lift Force}}{0.5\rho D\ell(A\omega_d)^2} \tag{20}$$

Sarpkaya [9] studied identically defined fluid lift force coefficients. He measured fluid lift forces directly acting on a fixed cylinder in an oscillating fluid flow field, and calculated the lift force coefficients. He said that for Reynolds number smaller than about 20,000,

the lift force coefficient depends primarily on Keulegan - Carpenter number, and in the Reynolds number range of from 20,000 to 100,000, the coefficient depends both on Reynolds and Keulegan - Carpenter number. But unlike Sarpkaya, this research deals with the lift force coefficient for an elastically mounted smooth cylinder exposed to an oscillating flow field. For an elastically mounted cylinder, it was found that the f_n/f_d ratio plays an important role in determining the force coefficient as well as both Reynolds and Keulegan - Carpenter numbers.

The experimental lift force coefficients were plotted against the f_{ns}/f_d ratios in Figures 20 to 22. The upper part of the figures shows the peak lift force coefficients while the lower part shows the R.M.S. lift force coefficients. As seen in the figures, the R.M.S. force coefficients exhibit the same functional dependence as the peak values.

Even though the experimental conditions are different, it is worthwhile to compare these results with Sarpkaya's data [9]. Figure 20 shows the case where Keulegan - Carpenter number was constant (K = 25.1) and the Reynolds number was varied by changing the cylinder driving frequency (f_d). The peak lift force coefficients ($C_{L(pk)}$) which Sarpkaya obtained for each corresponding Reynolds and Keulegan - Carpenter numbers were plotted as a dotted

line in the upper part of Figure 20. The dotted line matches quite well with the value of the peak lift force coefficient in this work when the f_{ns}/f_d ratio is around 3.3, 4.6, 5.6 and 7.4. It was found, in each of these regions where Sarpkaya's data matches with this experiment, that very low cylinder response amplitudes occurred as shown in the lower part of Figure 12. In other words, the lift force coefficients for an elastically mounted cylinder with very low response amplitudes are almost the same with those of a fixed cylinder. This fact indicates that this experiment and Sarpkaya's [9] experiment support each other.

It was also found that the cylinder vibration in y-direction generally increases the lift force coefficients. As shown in Figures 20 to 22, there is a trend that an integer f_{ns}/f_d ratio gives high cylinder response amplitudes and also a sharp increase of lift force coefficient especially, for the low Keulegan - Carpenter number region. It was observed that the lift force coefficient increases up to twice of that for a fixed cylinder in certain cases.

Practically, the maximum lift force coefficients are important in determining design loads. In Figure 23 and Figure 24, the maximum lift force coefficient is plotted against the Keulegan - Carpenter number. As drawn in the figures, both the maximum peak lift force coefficient (Max.

$C_{L(pk)}$) and the maximum R.M.S. lift force coefficient (Max. $C_{L(RMS)}$) decreases as the Keulegan - Carpenter numbers increase. Using nonlinear regression curve fitting techniques for the data points, empirical equations for the data were obtained to be

$$\text{Max. } C_{L(pk)} = 10.85\ K^{-0.36} \tag{21}$$

and

$$\text{Max. } C_{L(RMS)} = 4.45\ K^{-0.36} \tag{22}$$

Wilson [39] also obtained the maximum R.M.S. lift force coefficient for elastically mounted small tubes (D = 0.25 and 0.5 inch) in an oscillating fluid flow. He measured the cylinder R.M.S. response amplitudes, the effective mass of the cylinder, and the cylinder damping coefficient in order to obtain maximum lift force coefficient by an indirect means. Then, using a wake oscillator type of model, he also developed an empirical relationship for the maximum $C_{L(RMS)}$ value for his models. His empirical relationship was found to be

$$\text{Max. } C_L(RMS) = 3.69\ K^{-0.33} \tag{23}$$

This relationship is plotted in Figure 24 as '□' characters, and shows that the trend is almost identical with this experiment. The differences of Max. $C_{L(RMS)}$ value between Wilson's work and this experiment

appeared to be less than 10 per cent. When considering the very complicated fluid-structure interaction mechanism and the two different methods used to obtain the lift force coefficients, a 10 per cent variation shows good agreement. This experiment supports Wilson's results and the indirect method to calculate lift force coefficients that he introduced.

V. RESULTS

This study reveals several interesting facts about the self-induced cylinder vibrations due to an oscillating fluid flow.

These include:

1. Experimental results support the simple theoretical model of fluid lift forces acting on an elastically mounted cylinder as shown in Equation 11 for a range of Re (3,000 to 40,000) and K (15 to 120). There are three dominant peak frequency components in the directly measured fluid lift forces as predicted in the theoretical model of Equation 13. The three frequency components are one at the lower side band ($f_v - 2f_d$), one at the vortex shedding frequency (f_v), and one at an upper side band ($f_v + 2f_d$).

2. The natural frequency of an elastically mounted cylinder in y-direction has been found to vary with different operating conditions. As shown in Figures 7 and 8, the variation of the natural frequency due to cylinder response motion is very small (less than 1 per cent for 2-inch diameter cylinder). However, the natural frequency varies significantly with the nondimensional number V_R^* ($= \frac{Af_d}{Df_{ns}}$). When V_R^* is less than 0.95 the cylinder natural frequency is almost constant, but when V_R^* is greater than 0.95 the cylinder natural frequency increases

as V_R^* increases. The increase of the cylinder natural frequency can be explained by changes in the fluid added mass. As V_R^* increases, fluid added mass is reduced and in turn the cylinder natural frequency increases. In this experiment, a negative fluid added mass was not observed but a negative added mass can be anticipated for very high V_R^* numbers; i.e., V_R^* greater than about 1.56 for 2-inch cylinder.

3. Whether a cylinder in periodic fluid flow is fixed or free to respond in y-direction, it was found that the Strouhal number (S_t) does not remain constant near 0.2 as in the steady fluid flow case, but, rather drops into the narrow range of from 0.15 to 0.20, except in locked-on region where S_t is greater than 0.2. For the low Keulegan - Carpenter number region (Low A/D ratio; A/D < 12) an integer f_v/f_d ratio was always found, on the other hand for the high Keulegan - Carpenter nlmber (high A/D ratio; A/D > 12), a fractional f_v/f_d ratio appeared. That is because, for the case of a low A/D ratio, a shedding vortex is not either significantly dissipated or moved when the cylinder returns to that position. Then, as shown in Figure 1, a strong and consistent vortex shedding spatial pattern can be easily formed. The consistent vortices and spatial pattern make the f_v/f_d ratio to be an integer. On the other hand, a large A/D ratio makes relatively inconsistent

vortex sheddings compare with the case of a low A/D ratio. In this case the wakes are almost dissipated or easily move away when the cylinder returns, giving a fractional f_v/f_d ratio. It was also noticed that the vortex shedding frequency (f_v) increases as the Keulegan - Carpenter number (K) increases like Sarpkaya [9] and Bidde [38] had already observed.

4. Locked-on phenomenon was extensively observed in this experiment. As the cylinder vibrates in the y-direction, in a certain region (especially around mid f_n/f_d ratio region for each A/D ratio) the vortex shedding frequency (f_v) was changed to be the cylinder response frequency (f_r). Especially when the cylinder responds at its natural frequency ($f_r = f_n$), this type of locked-on behavior was easily observed around an integer f_n/f_d ratio for a wide range of Keulegan - Carpenter number. This locked-on condition gives a sharp increase in the cylinder responses and the fluid lift forces compared to the cylinder motion in uniform fluid flow.

Another interesting phenomenon, which was observed only in this oscillating fluid flow is a strong tendency for the f_r/f_d ratio to be an integer when f_n/f_d was also near an integer ratio. In other words, the cylinder response frequency (f_r) changed so that the f_r/f_d would be an integer even when this cylinder response frequency (f_r) is

different from the cylinder natural frequency (f_n). This tendency to form closed cylinder motion paths like that shown in Figure 1, around an integer f_n/f_d ratio, can be viewed as a type of locked-on behavior. In this case, however, the change in the cylinder response frequency (f_r) from the cylinder natural frequency (f_n) corresponds to a sharp decrease in both the amplitudes of cylinder response and the fluid lift force. This type of locked-on (closed spatial loop of the cylinder path) behavior was only observed for low A/D ratios ($A/D \leq 10$). For high A/D ratios, it was hard to obtain a consistent vortex sheddings situation as explained previously. This indicates that it is not natural to have a closed cylinder path in a high A/D ratio region.

5. The relationships between the vortex shedding frequency (f_v), the cylinder response frequency (f_r), and the cylinder natural frequency (f_n) were observed.

First, in lower f_n/f_d ratio region which corresponds to the higher cylinder driving case, the vortex shedding frequency (f_v) is always higher than the cylinder response frequency (f_r) and the cylinder natural frequency (f_n). For most of the cases in this region the $f_r = f_v - 2f_d$ relationship was maintained. In other words, the main excitation frequency (the vortex shedding frequency) mismatches with the response frequency (the cylinder response frequency) by two times the cylinder driving frequency (f_d). As discussed in the

lift force model, the lower side band of the fluid lift force excites the cylinder in this lower f_n/f_d region.

Second, in mid f_n/f_d ratio region, the vortex shedding frequency (f_v) always matches with the cylinder response frequency (f_r). The cylinder motion and the vortex shedding interact strongly to support each other, giving strong spatially stable vortices and large amplitude of the cylinder response. In this case, the cylinder response frequency (f_r) and the cylinder natural frequency have little or insignificant differences. This phenomenon corresponds to the main locked-on condition. Even in this locked-on region, if the cylinder response frequency (f_r) differs from the natural frequency of the cylinder in order to form the closed spatial cylinder paths, the cylinder response amplitude drops significantly. This phenomenon corresponds to another type of locked-on behavior.

Third, in upper f_n/f_d ratio region, which corresponds to a low driving frequency case, the vortex shedding frequency (f_v) is always lower than the cylinder response frequency (f_r) except for several special locked-on cases. This difference between the vortex shedding frequency (f_v) and the cylinder response frequency (f_r) make relatively weak vortices compared with the lower and mid f_n/f_d ratio regions. Very low cylinder responses were observed in this region even for the locked-on cases.

This case corresponds to the vortex shedding frequency plus twice the cylinder driving frequency.

6. It is believed that certain combinations of several factors such as the vortex strength, the cylinder response frequency (f_r), the cylinder natural frequency (f_n), the f_n/f_d ratio, and the f_r/f_d ratio ...etc. determines cylinder response amplitudes. It was known that in case of a steady fluid flow, the cylinder response jumps up in locked-on region when $f_n = f_v$. In the oscillating fluid flow case, the f_n/f_d ratio and the f_r/f_d ratio play an extremely important role in determining the cylinder responses. When $f_n/f_d = f_r/f_d = f_v/f_d$ are equal and integer values, the highest cylinder response amplitude occurs.

As explained previously, the cylinder response amplitudes are self-limiting due to the size of vortices and relative spatial locations. The observed maximum cylinder response amplitude was about 1.0 D to 1.15 D peak to peak. The maximum cylinder response amplitudes were observed to decrease as the Keulegan - Carpenter number increased.

Practically, the most interesting point is how to reduce the structure vibration amplitude in actual fluid-structure problems. An idea can be suggested from this experiment. When V_R ($= \frac{Af_d}{Df_n}$) is less than around 0.6, the cylinder response amplitude is reduced. It was found

that when $V_R \leq 0,6$, the cylinder vibration is very low even for the locked-on cases.

7. It was known that for a fixed cylinder in a periodic fluid flow, the fluid lift force coefficient depends both on Reynolds number and Keulegan - Carpenter number. For the elastically mounted cylinder in an oscillating fluid flow, it was found that the fluid lift force coefficient depends on its f_n/f_d ratio as well as an Re and K. A very high fluid lift force coefficient was measured around an integer f_n/f_d ratio and low Keulegan - Carpenter number region. The maximum lift force coefficient (Max. C_L) was found to decrease as the Keulegan - Carpenter number increases in a manner similar to the cylinder response amplitude. The statistical nonlinear regression lines for a maximum lift force coefficient were obtained as

$$\text{Max. } C_{L(pk)} = 10.85\ K^{-0.36} \tag{21}$$

and

$$\text{Max. } C_{L(RMS)} = 4.45\ K^{-0.36} \tag{22}$$

These results for the maximum fluid lift force coefficient matches quite well, within 10 per cent difference, with Wilson's [39] results as shown in Figure 24. Considering the fact that Wilson [39] obtained the R.M.S. lift force coefficient by an indirect method, a 10 per cent difference is considered to be insignificant.

It was found that the peak and R.M.S. force coefficients, as defined in Equations 19 and 20, show the same functional dependence. In addition, the cylinder response motion in y-direction has a good correlation with the fluid lift force coefficient. This means that the cylinder response amplitude as well as the R.M.S. and peak lift force coefficients can be used as a tool to measure the fluid-structure interaction phenomenon in an oscillating fluid flow.

VI. CONCLUDING REMARKS

This study started from the question, "What happens when an elastically mounted circular cylinder is exposed to periodic fluid flow?" The experimental study showed that the cylinder responses in the y-direction affect vortex formation behind the cylinder and, in turn, influence the fluid lift forces acting on the cylinder. It was known that the fluid lift forces acting on a fixed cylinder due to periodic fluid flow are dependent on Reynolds and Keulegan-Carpenter numbers. On the other hand, a new fact was found in this experiment for an elastically mounted cylinder in an oscillating fluid flow field. The fact is a combination of frequency components, which include the cylinder natural frequency f_n, the cylinder response frequency f_r, the cylinder driving (input) frequency f_d, and the vortex shedding frequency f_v, can be used to explain the resulting locked-on phenomenon, the cylinder responses in the y-direction, and the fluid lift forces. It was noticed that f_n/f_d ratio plays a more important role in determining the cylinder response amplitude and the fluid lift forces than either Reynolds and Keulegan-Carpenter numbers. This research work places great emphasis on a close examination of all the frequency components of interest in order to explain the experimental data; namely, to predict the fluid lift forces and the

cylinder response amplitudes in the y-direction. Also the vortex shedding frequency f_v, and Strouhal number S_t, were examined in order to see the interaction between the cylinder motion and the vortices generated behind the cylinder. The question, "What happens?", was answered through this experiment only in the sense that we are now able to anticipate what will happen under similar fluid-structure interaction problems. Also we can say under which conditions the cylinder response motion interacts with the vortex formations and leads to a locked-on phenomenon which should be avoided in actual structure design procedures.

During the course of the experiment, several additional topics of interest requiring further study emerged.

These topids are:

1) In this work, only two different sized cylinder models were used. The effect of the cylinder diameter on the cylinder natural frequency variation, the cylinder response amplitudes, ...etc. needs to be examined for a wider range of cylinder diameters.
2) The installation of a two-axis dynamic force transducer would allow the fluid drag forces as well as the fluid lift forces to be measured simultaneously. It is necessary to analyze the fluid drag forces about an elastically

mounted cylinder and to compare these results to the fixed cylinder case in order to establish the effect of cylinder response on the drag forces.

3) By placing the circular cylinder near the water tank wall, the blockage effect could be tested using this experimental apparatus.
4) This experiment was performed in the range of the Reynolds numbers less than 40,000 and the Keulegan-Carpenter numbers less than 120. It is important to study this fluid structure interaction problem for Reynolds numbers and Keulegan-Carpenter numbers that are in the range encountered in the field for large structures and/or structural components. In other words, some large scale verification tests need to be conducted to verify that similar behavior occurs in large structures.

VII. FIGURES

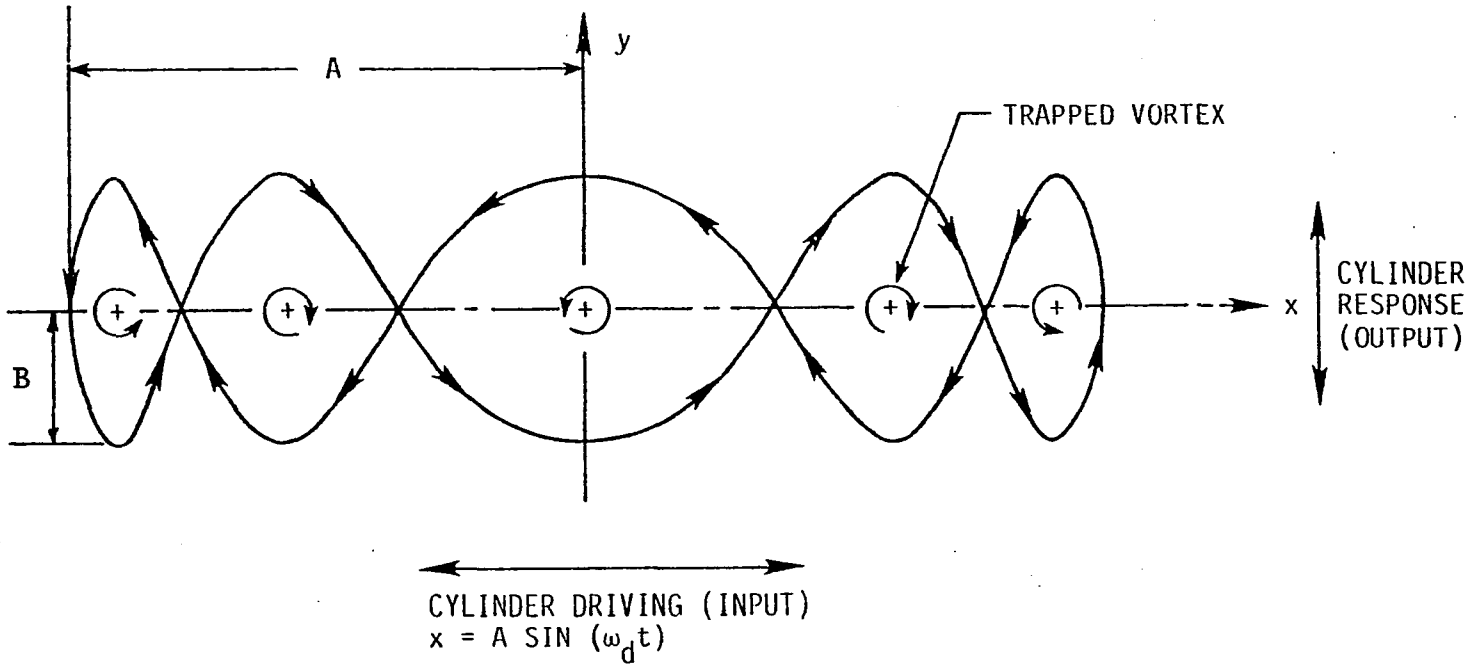

Figure 1. An example of Lissajour loop of cylinder motion when $f_r/f_d = 5$

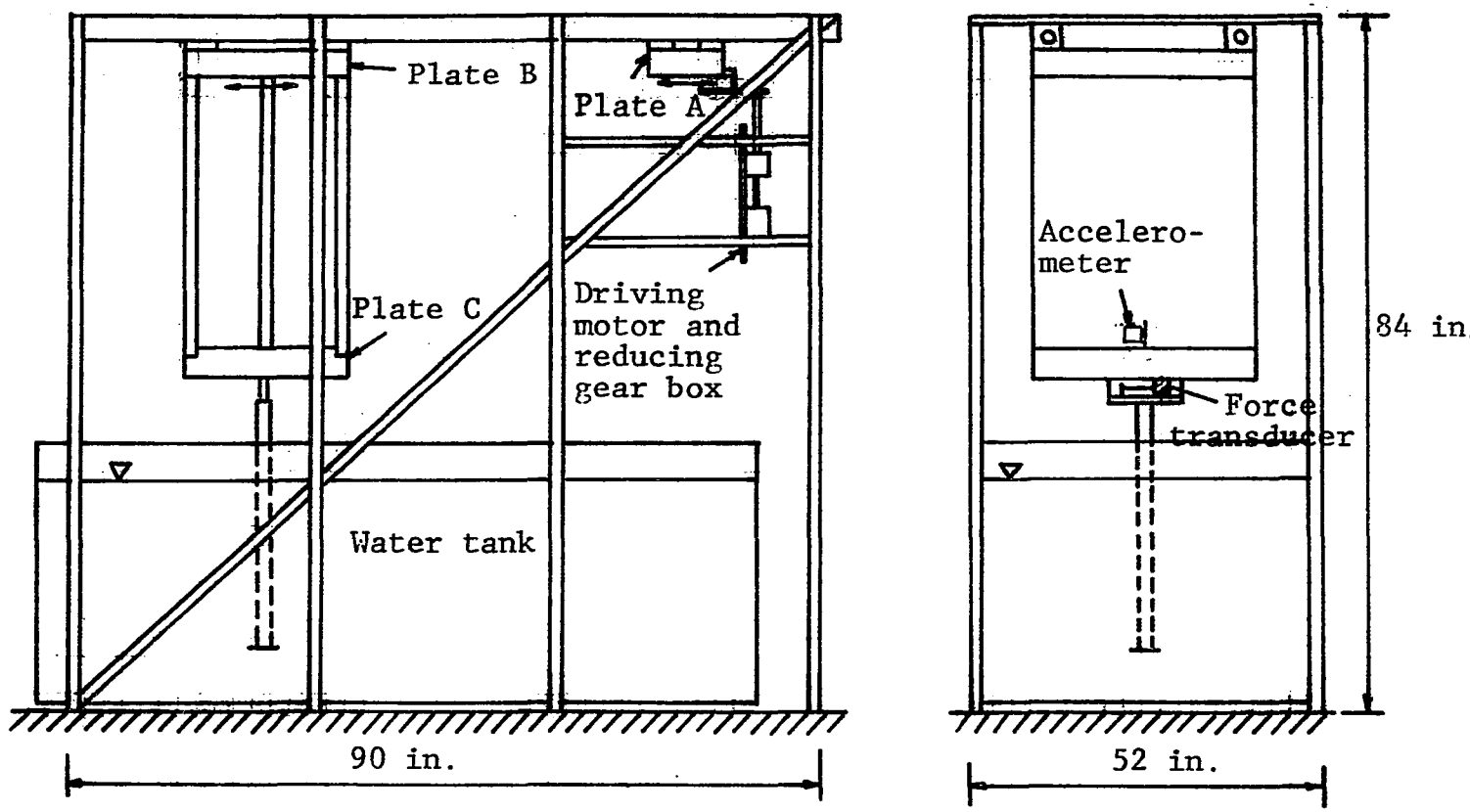

Figure 2. Schematic of the experimental apparatus

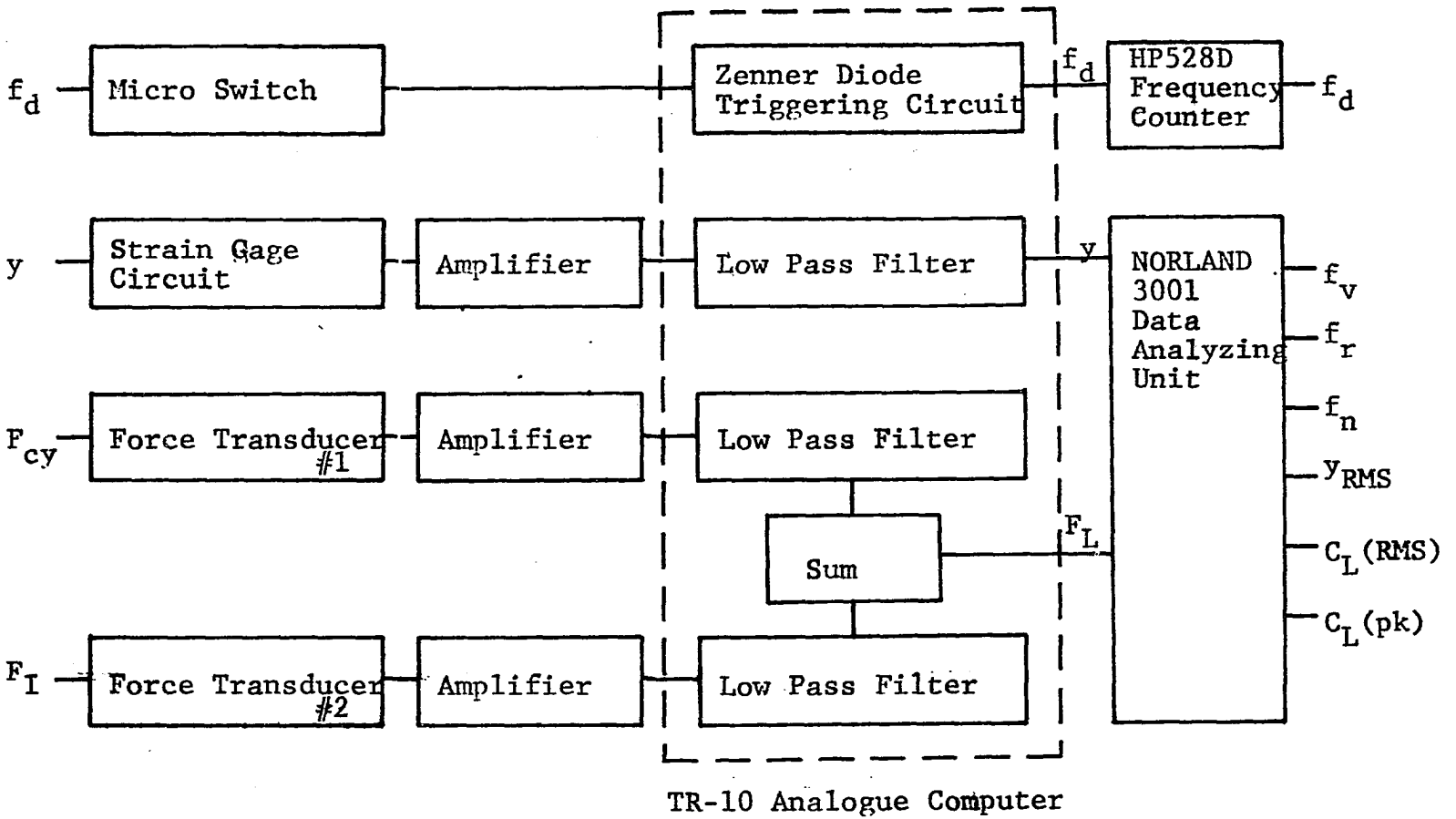

Figure 3. Schematic diagram of data acquisition system

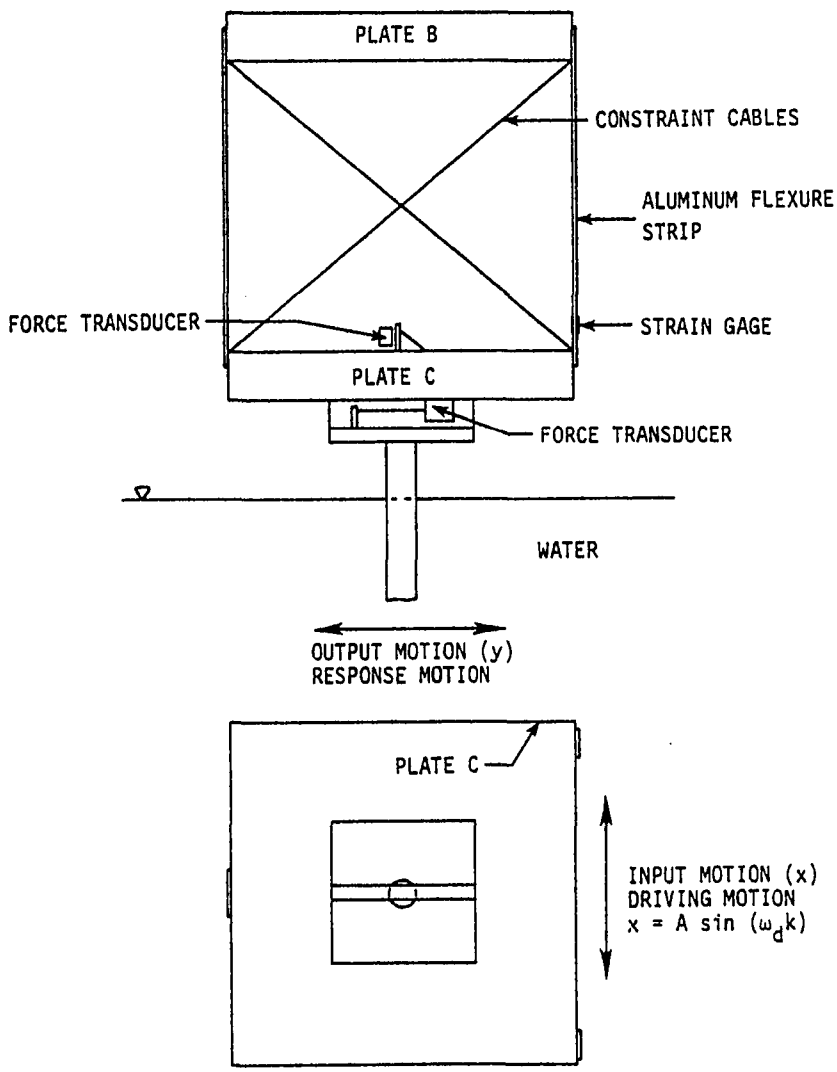

Figure 4. Schematic of cylinder structure showing input (driving) and output (response) directions

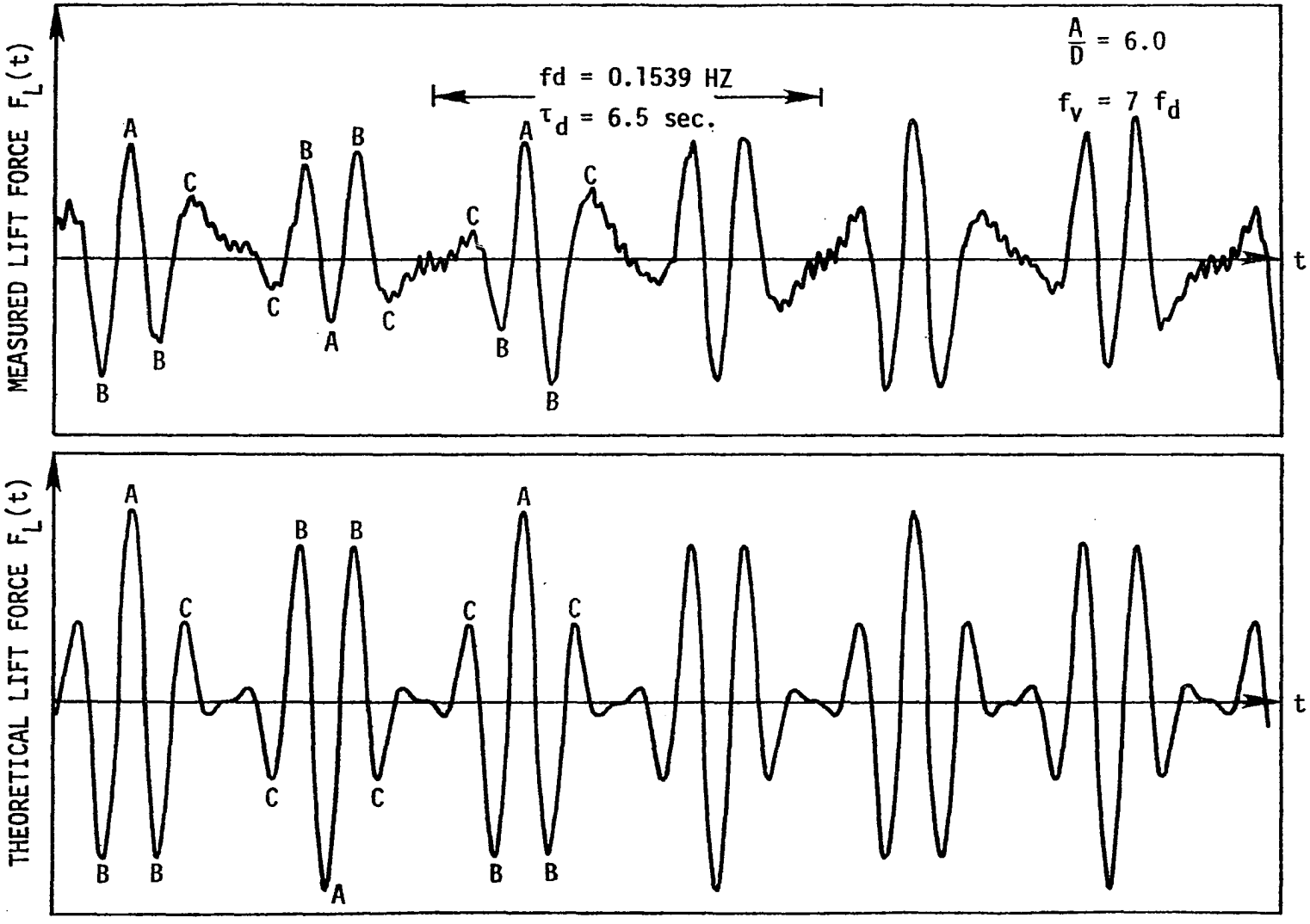

Figure 5. A typical measured and theoretical fluid lift force time history for constrained output motion

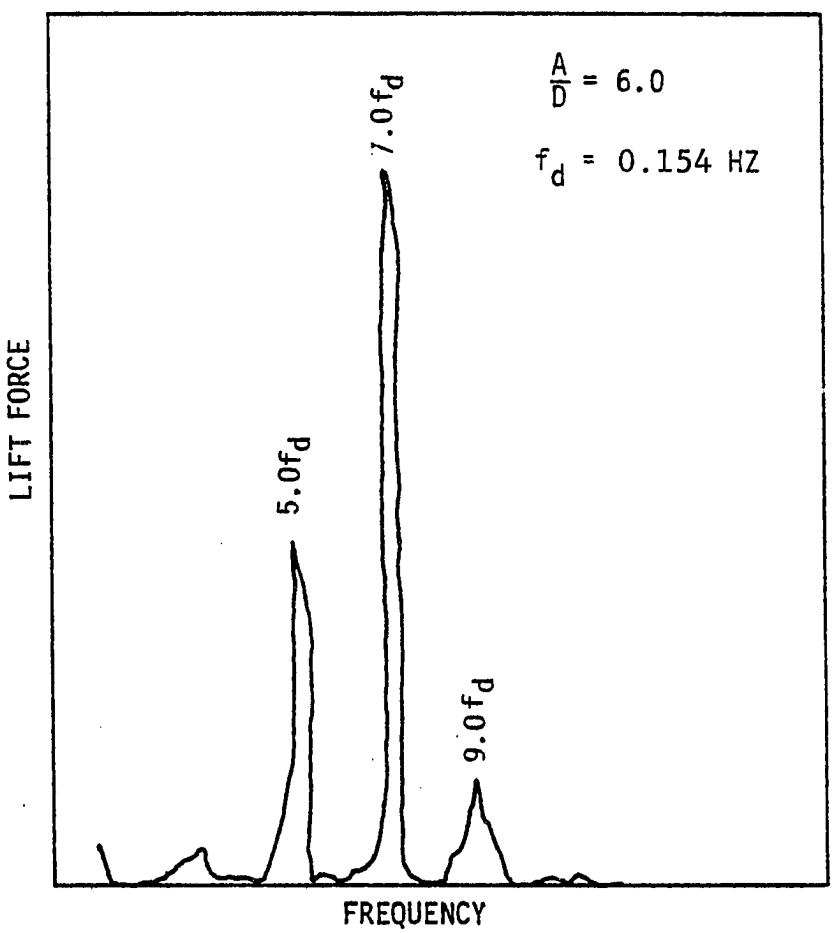

Figure 6. Frequency analysis of the measured fluid lift force time history when A/D = 6.0 and f_d = 0.154 Hz

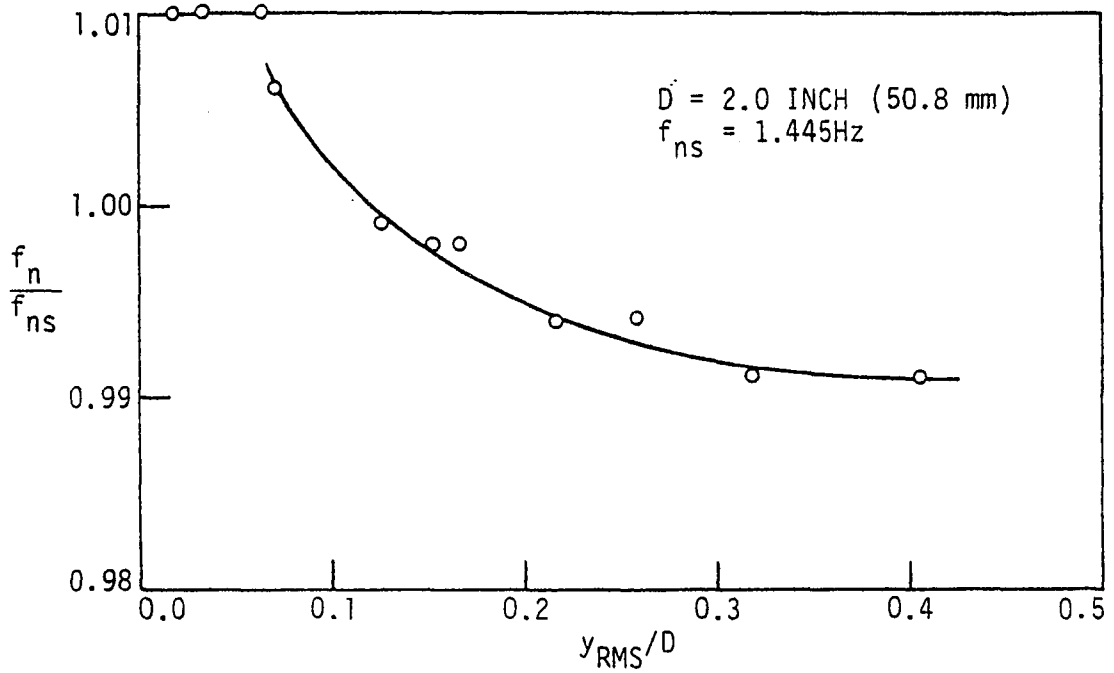

Figure 7. f_n/f_{ns} vs y_{RMS}/D for D = 2 inch

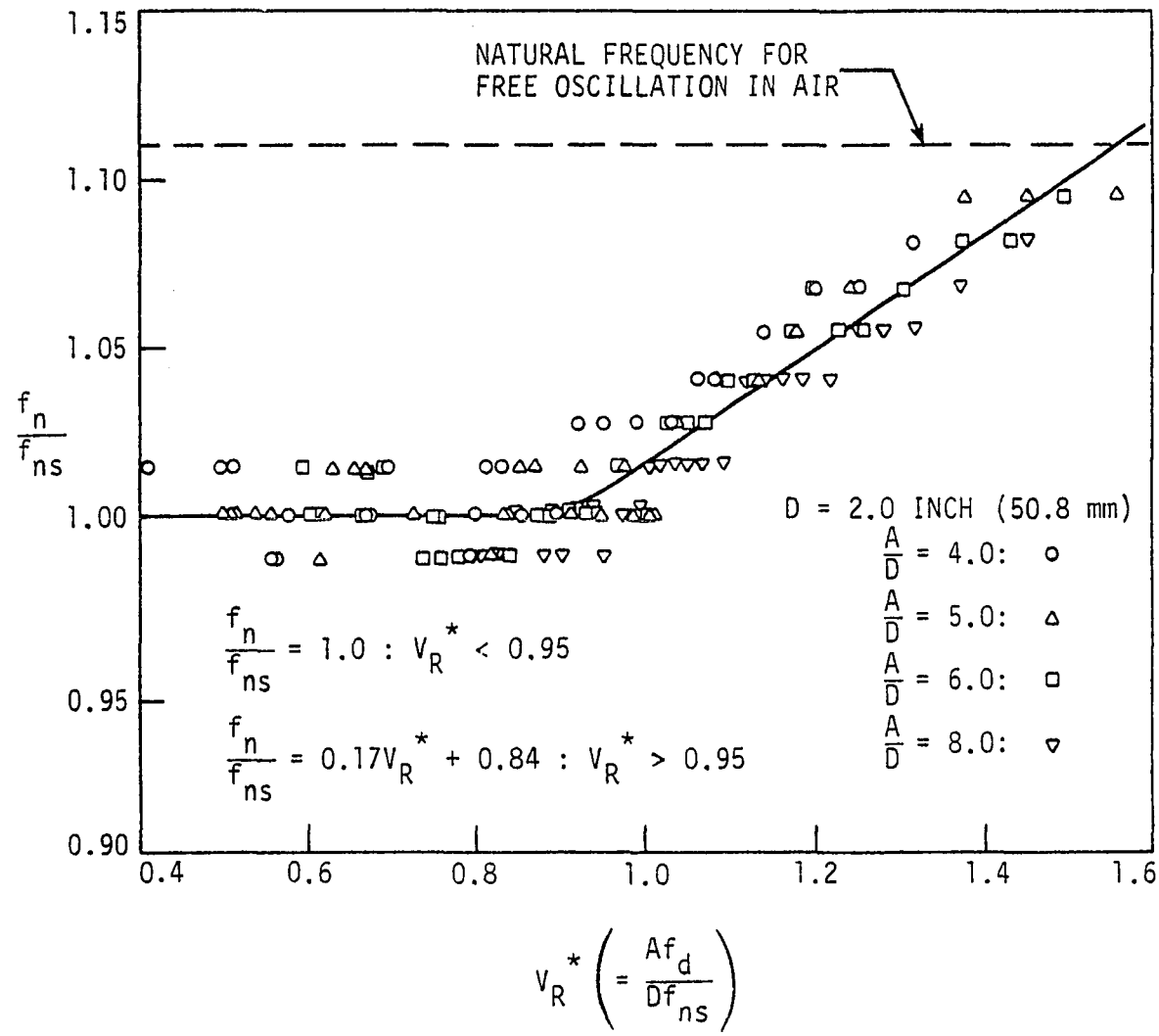

Figure 8. f_n/f_{ns} vs $V_R^*(= \frac{Af_d}{Df_{ns}})$ for D = 2 inch

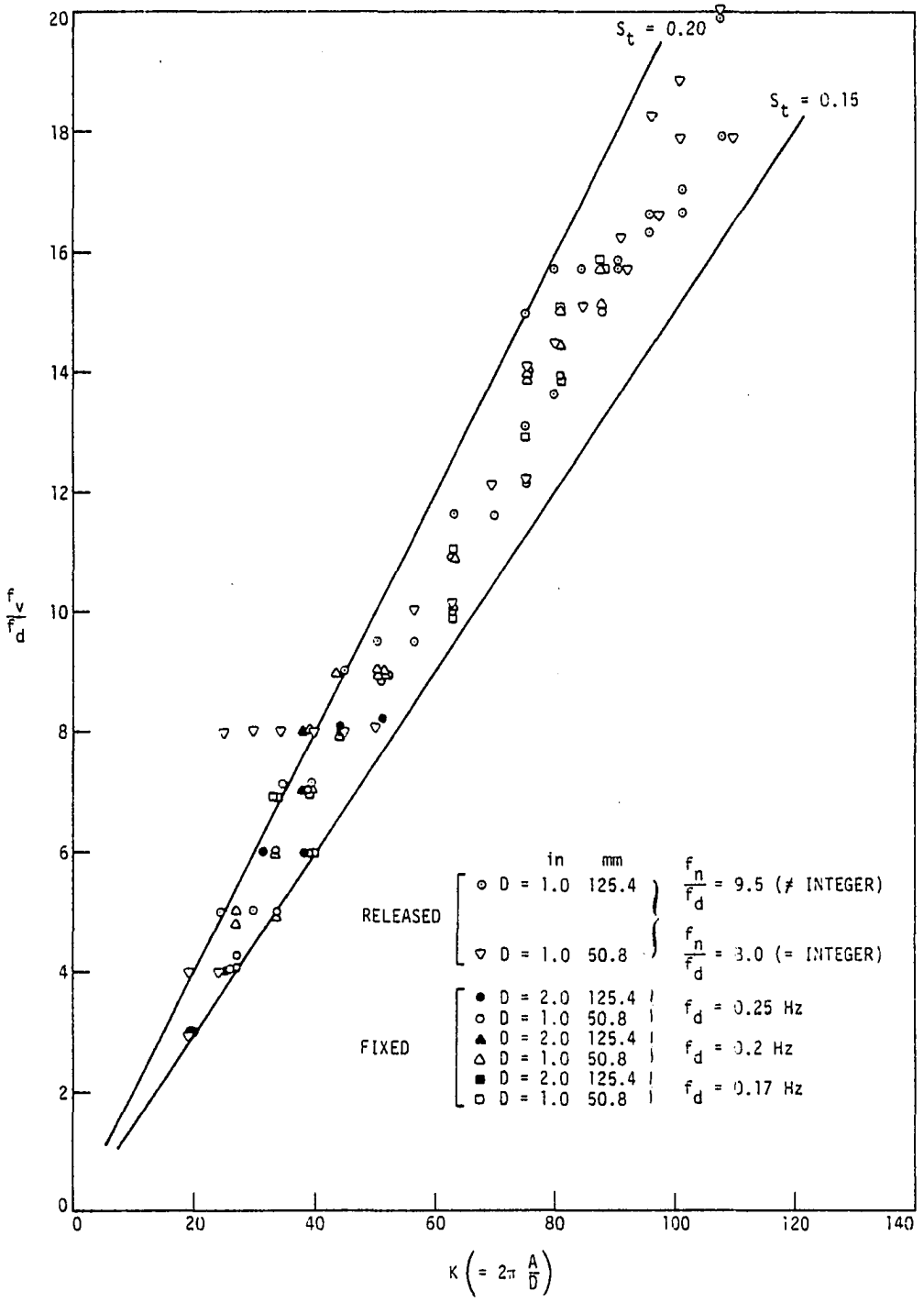

Figure 9. f_v/f_d vs K(= $2\pi\frac{A}{D}$)

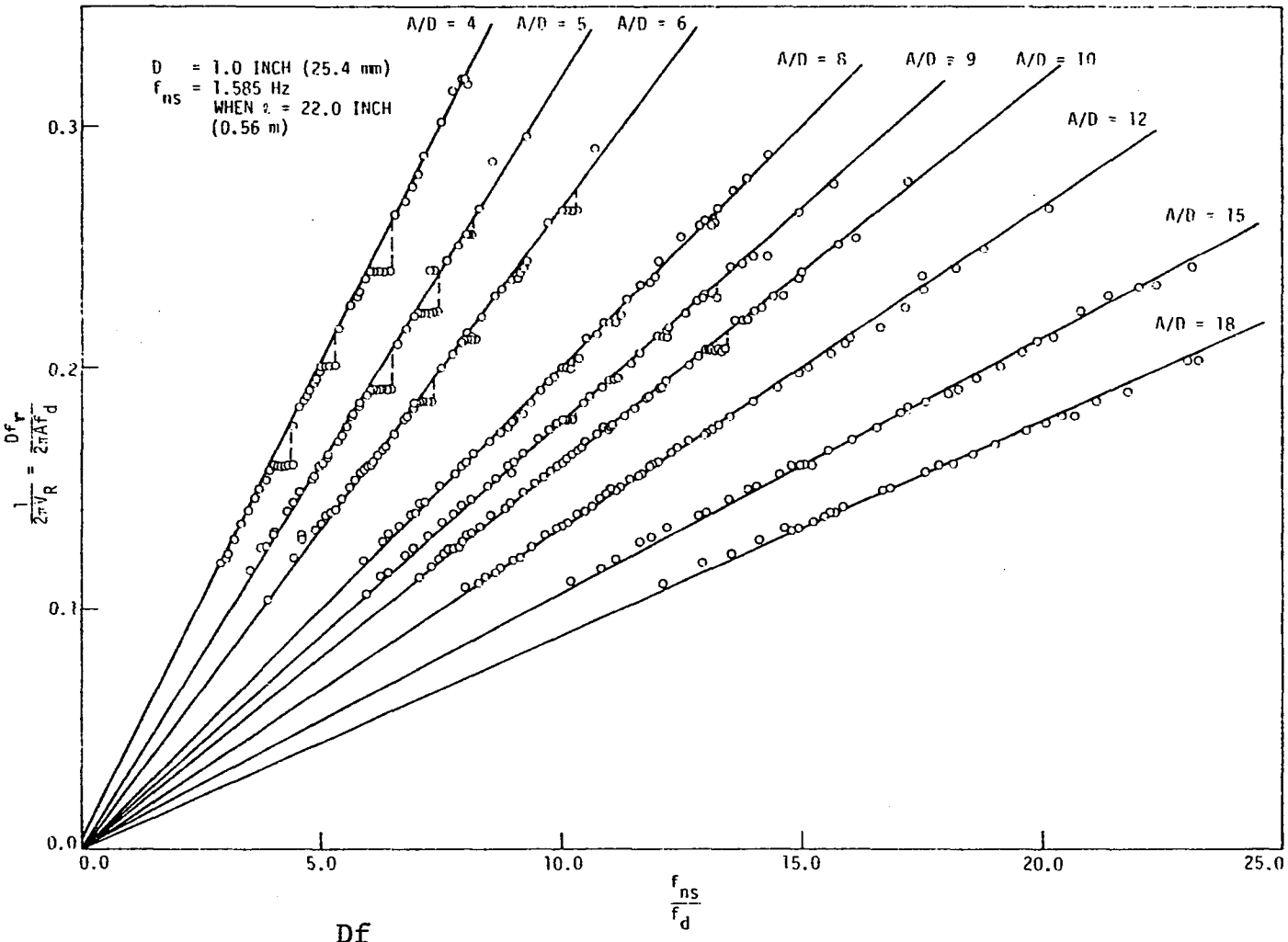

Figure 10. $1/(2\pi V_R)(= \frac{Df_r}{2\pi A f_d})$ vs f_{ns}/f_d for D = 1 inch and varying A/D ratio

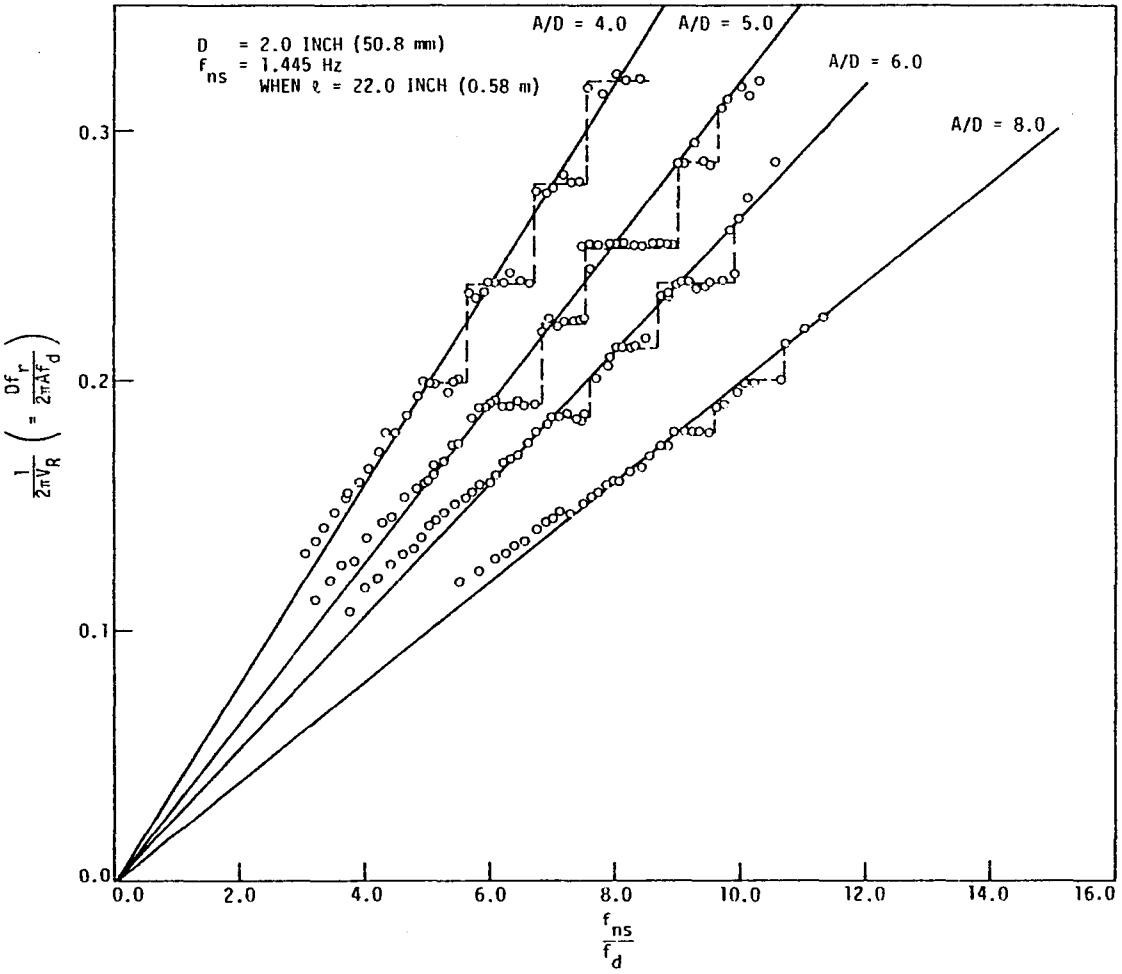

Figure 11. $1/(2\pi V_R)(= \frac{Df_r}{2\pi A f_d})$ vs f_{ns}/f_d for D = 2 inch and varying A/D ratio

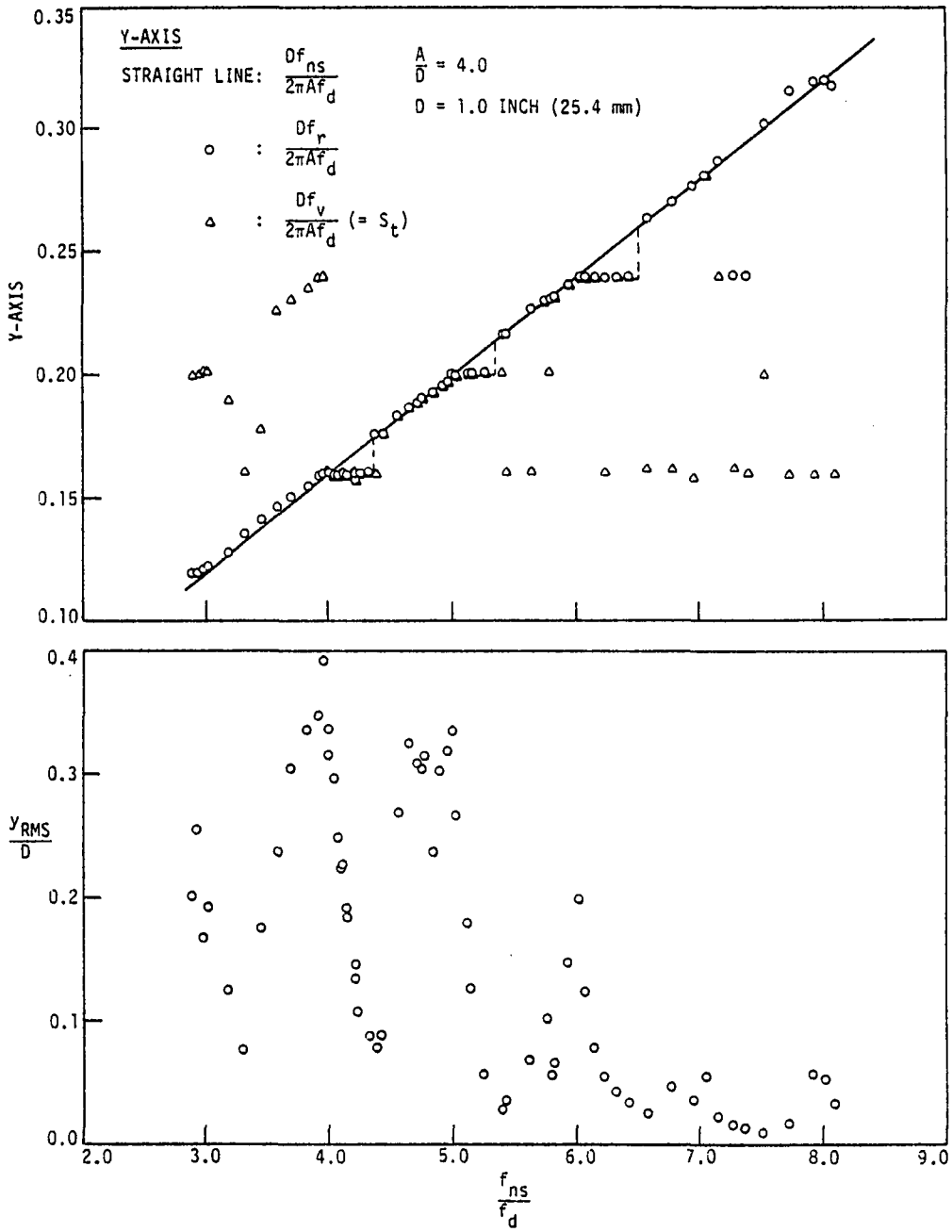

Figure 12. Frequency relationships between f_r, f_n, f_v and cylinder response amplitudes (y_{RMS}/D) for D = 1 inch and A/D = 4

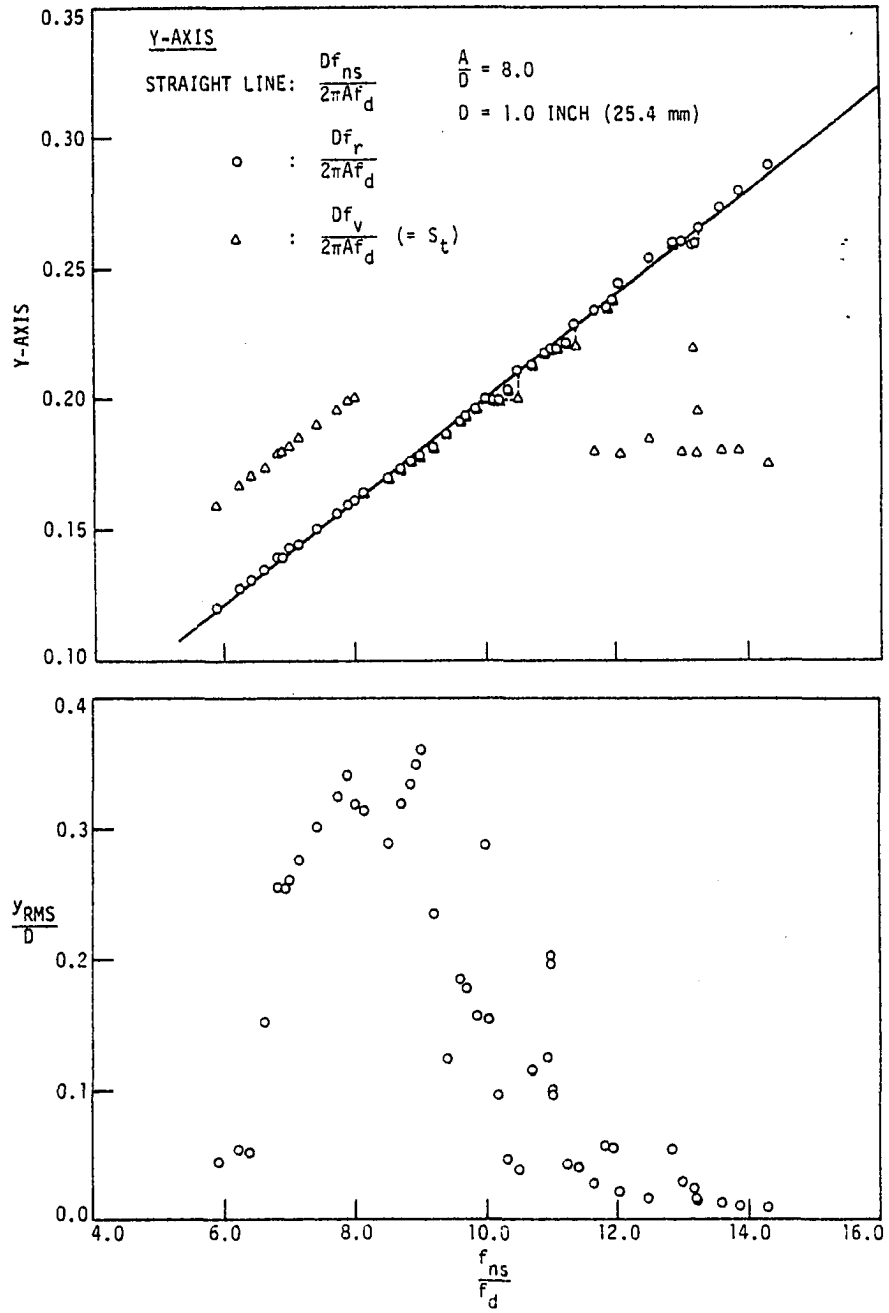

Figure 13. Frequency relationships between f_r, f_n, and f_v and cylinder response amplitudes (y_{RMS}/D) for D = 1 inch and A/D = 8

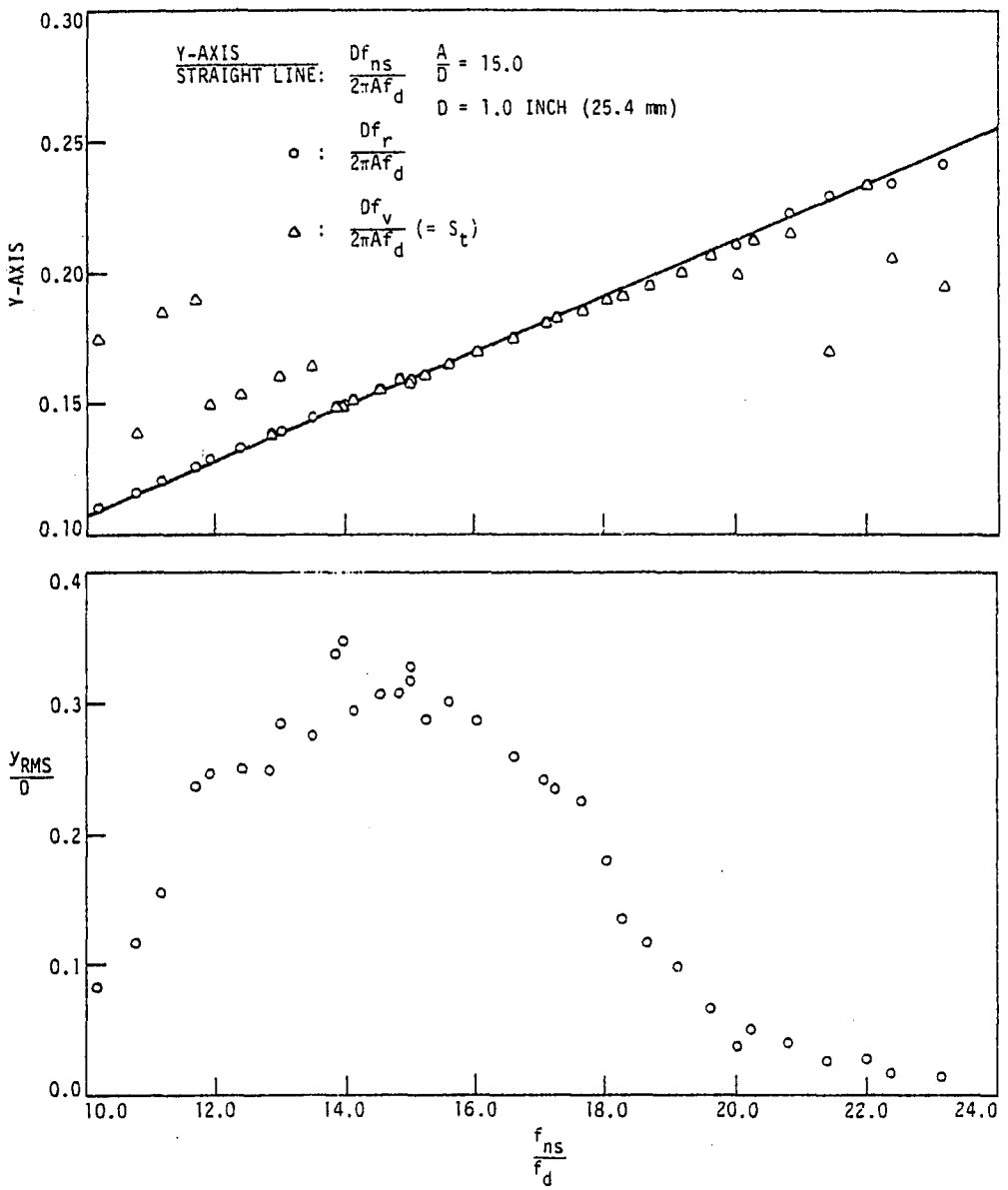

Figure 14. Frequency relationships between f_r, f_n, and f_v and cylinder response amplitudes (y_{RMS}/D) for D = 1 inch and A/D = 15

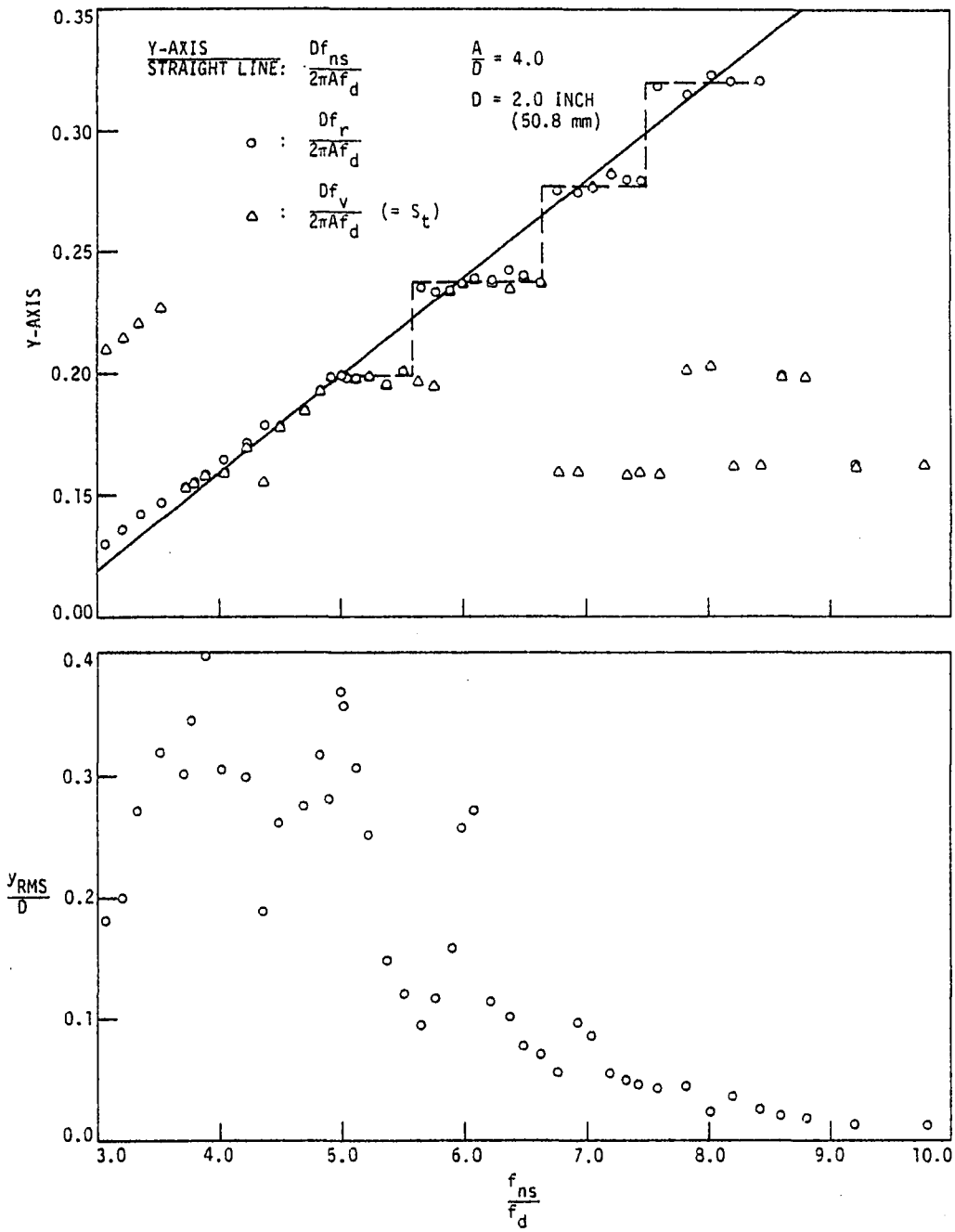

Figure 15. Frequency relationships between f_r, f_n, and f_v and cylinder response amplitudes (y_{RMS}/D) for D = 2 inch and A/D = 4

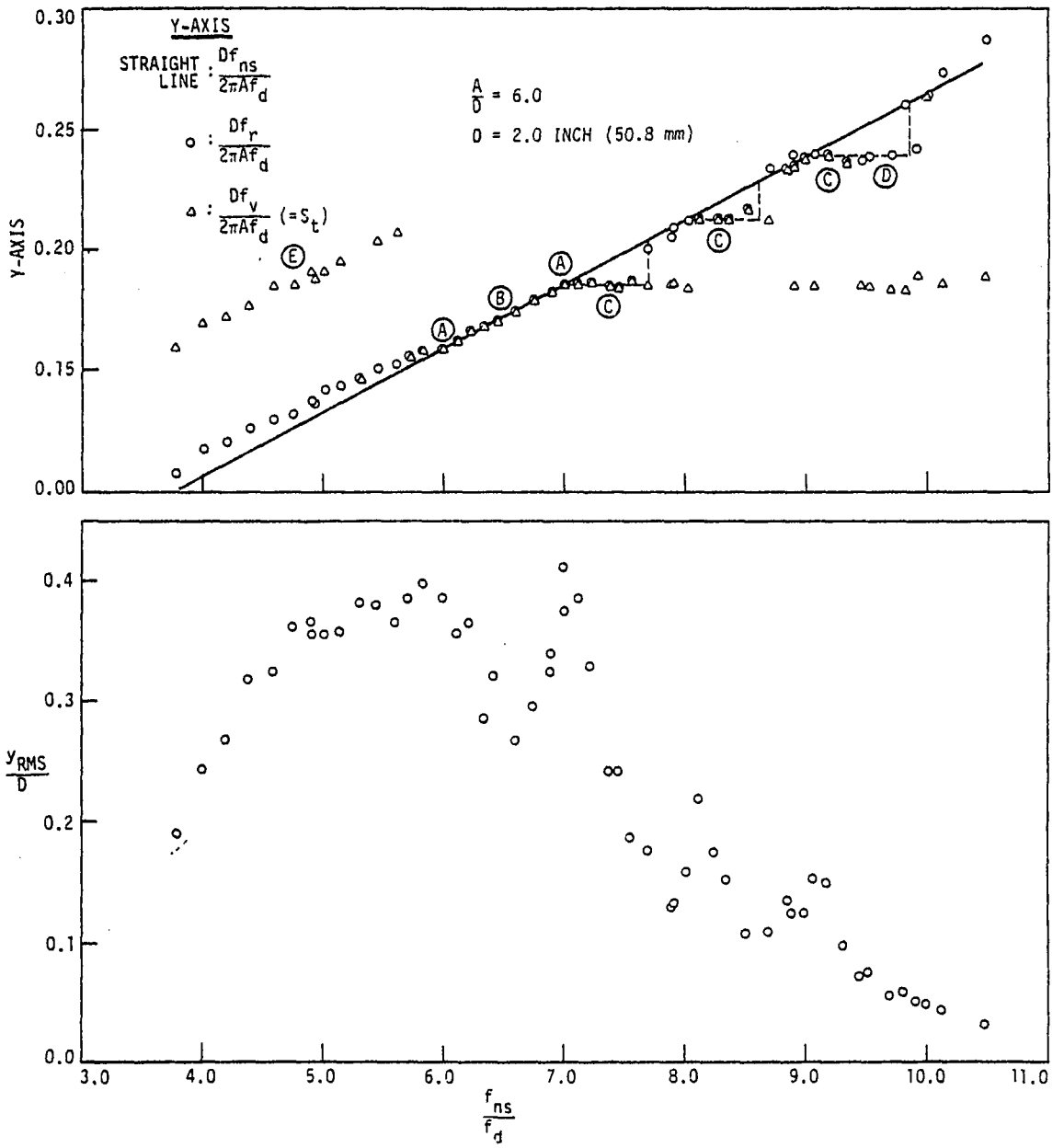

Figure 16. Frequency relationships between f_r, f_n, and f_v and cylinder response amplitudes (y_{RMS}/D) for D = 2 inch and A/D = 6

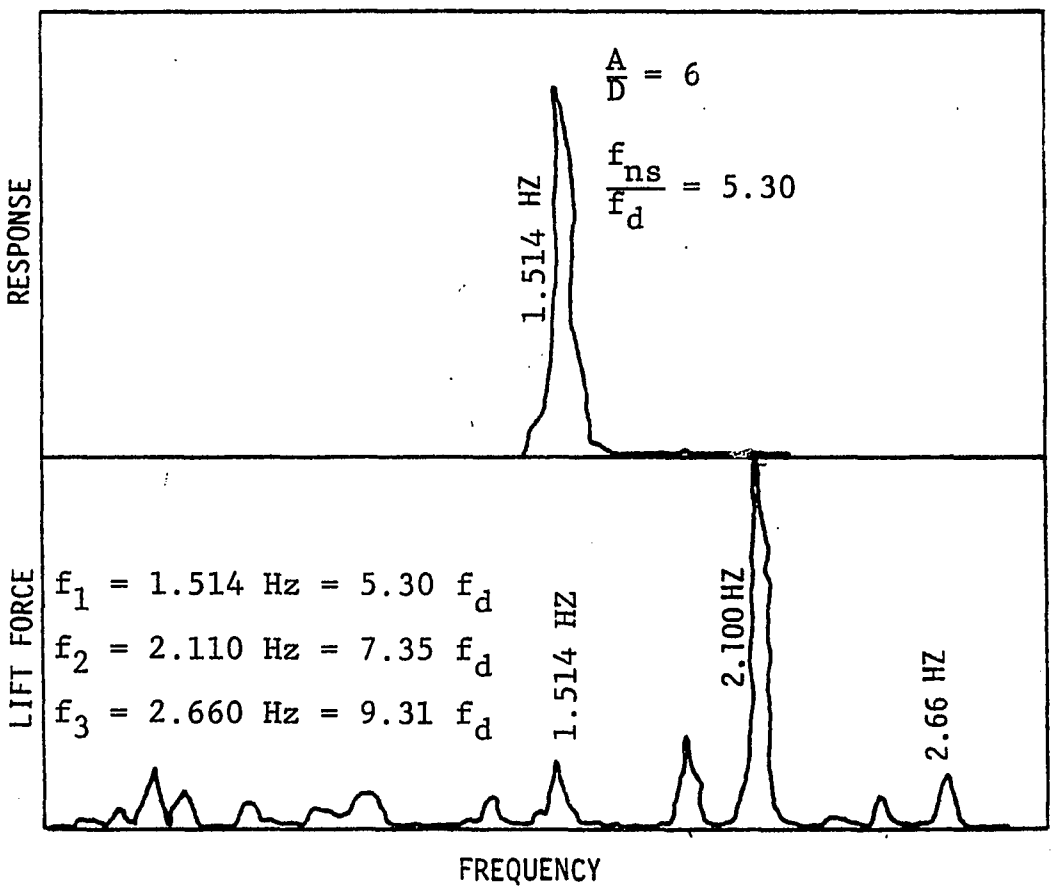

Figure 17. A typical frequency analysis of cylinder response and fluid lift force signal for lower f_{ns}/f_d ratio region (A/D = 6 and f_{ns}/f_d = 5.30)

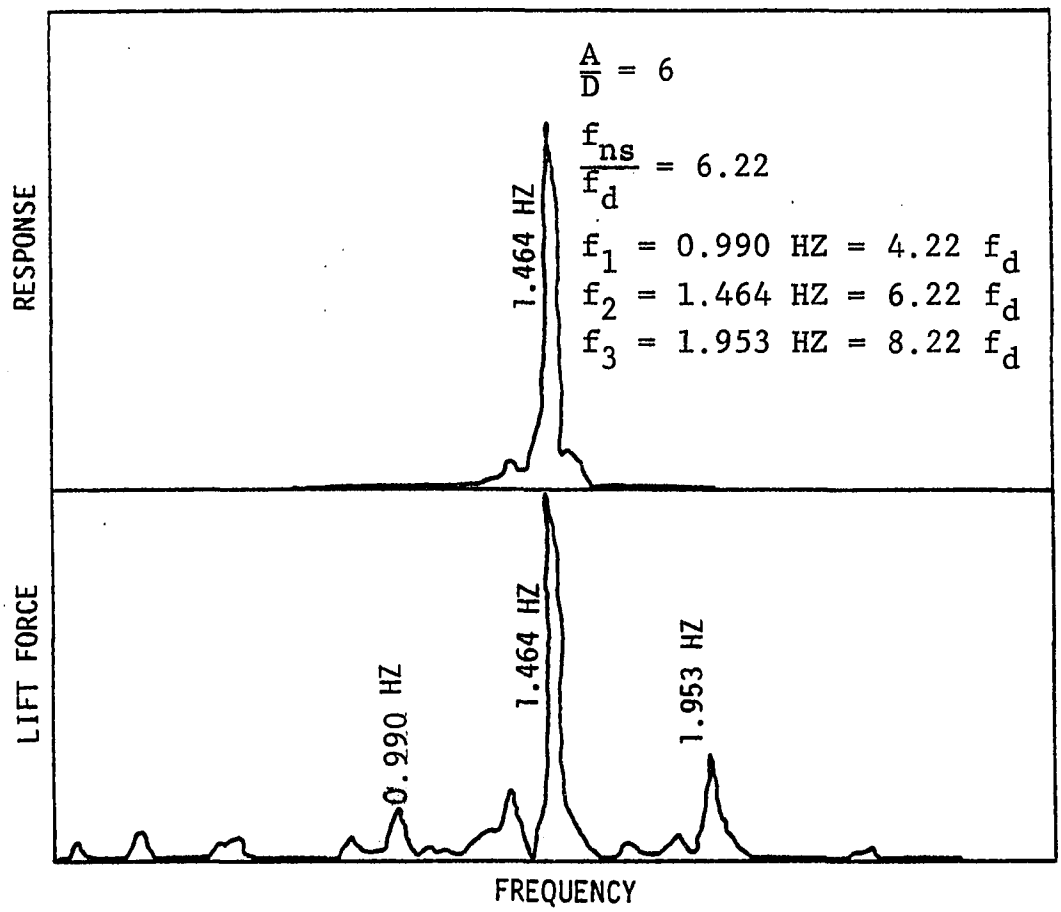

Figure 18. A typical frequency analysis of cylinder response and fluid lift force signal for mid f_{ns}/f_d ratio region (A/D = 6 and f_{ns}/f_d = 6.22)

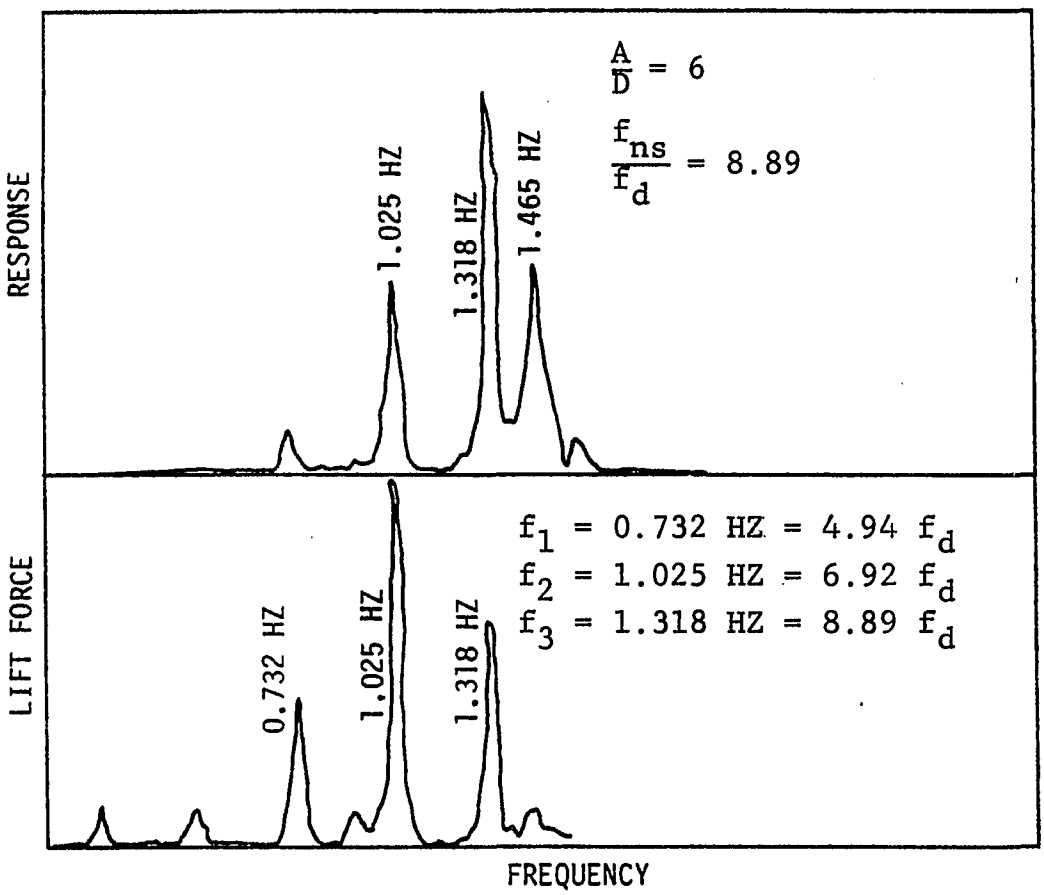

Figure 19. A typical frequency analysis of cylinder response and fluid lift force signal for upper f_{ns}/f_d ratio region (A/D = 6 and f_{ns}/f_d = 8.89)

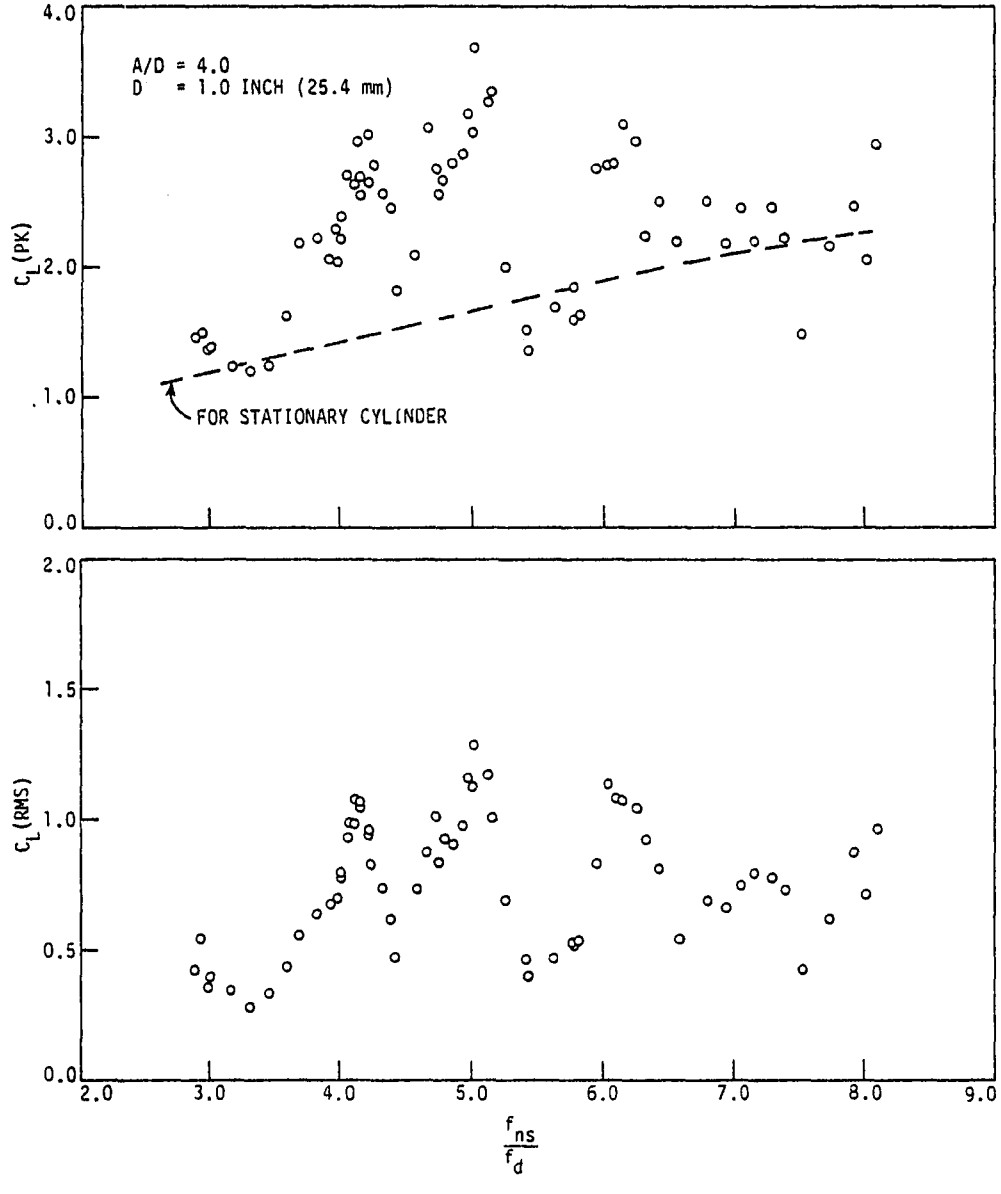

Figure 20. Lift force coefficient (C_L[pk] and C_L[RMS]) vs f_{ns}/f_d when D = 1 inch and A/D = 4

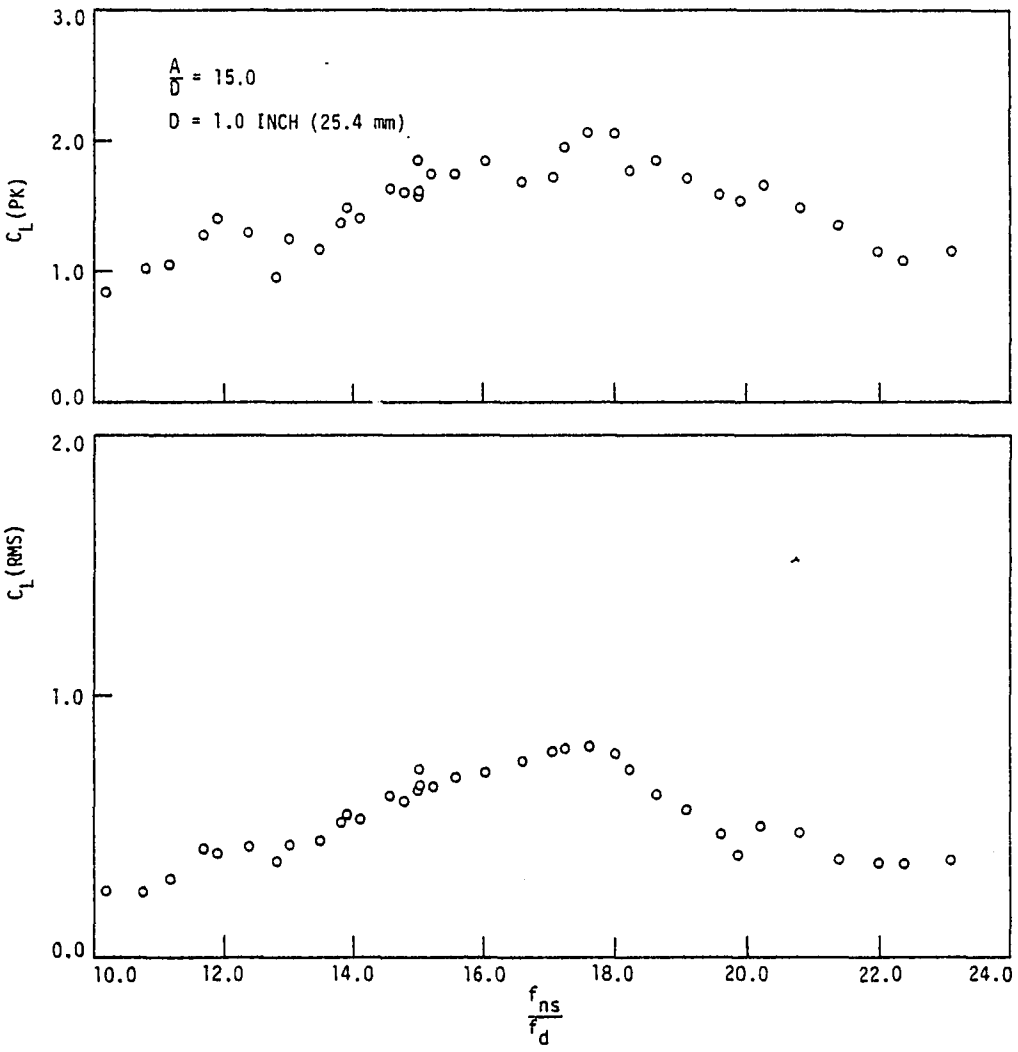

Figure 21. Lift force coefficient (C_L[pk] and C_L[RMS]) vs f_{ns}/f_d when D = 1 inch and A/D = 15

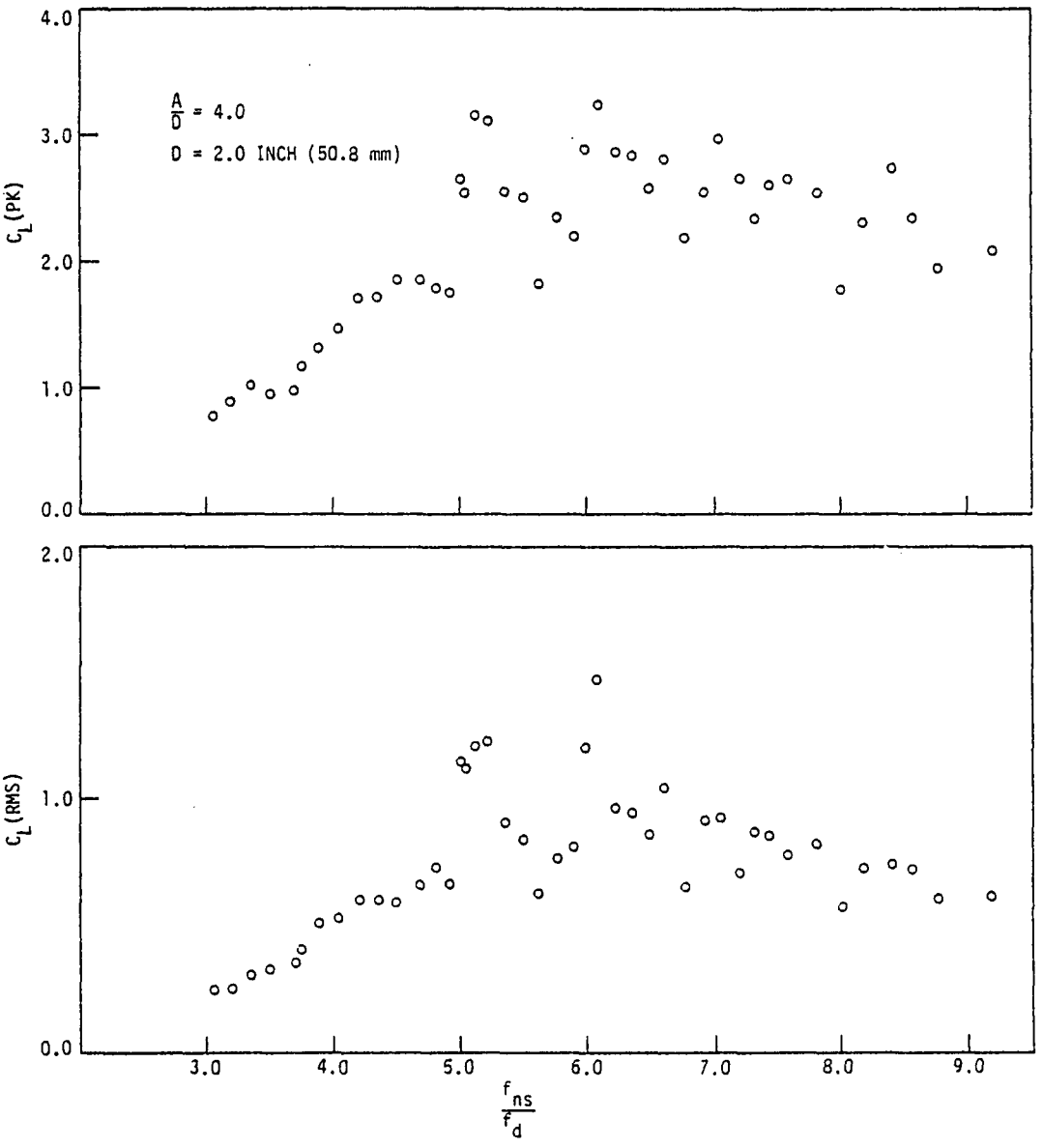

Figure 22. Lift force coefficient (C_L[pk] and C_L[RMS]) vs f_{ns}/f_d when D = 2 inch and A/D = 4

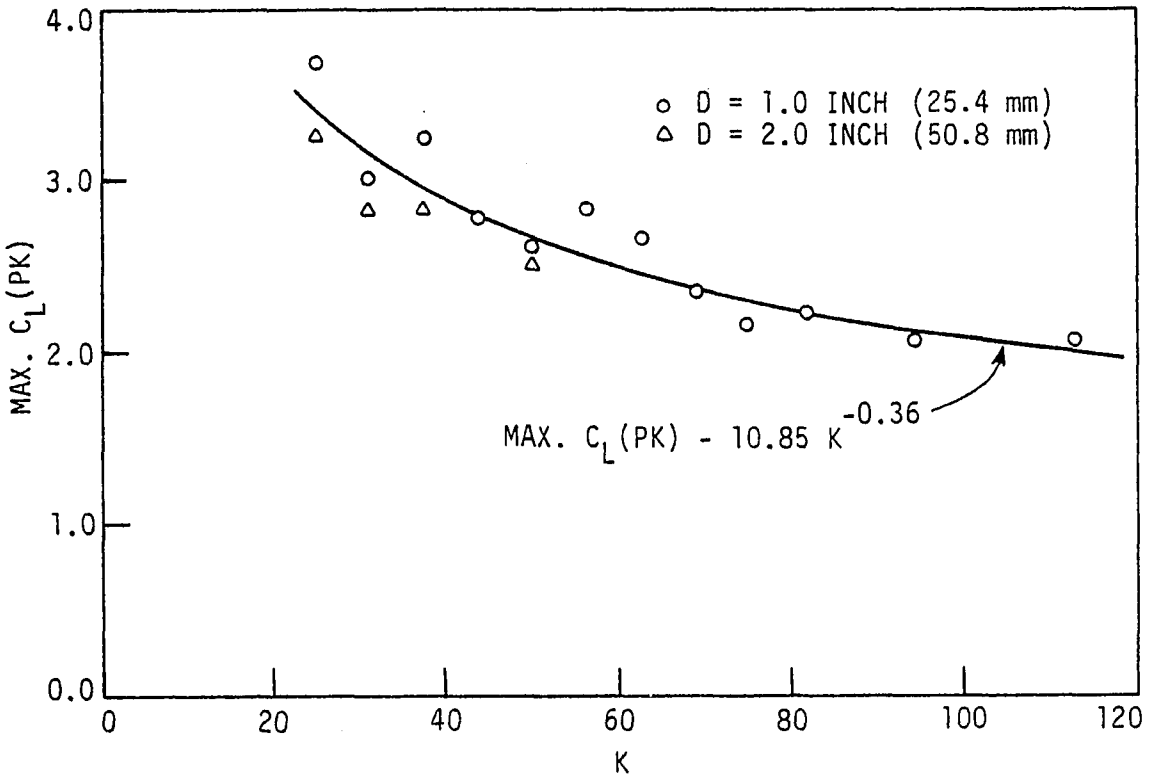

Figure 23. Maximum C_L(pk) vs K ($=2\pi\frac{A}{D}$)

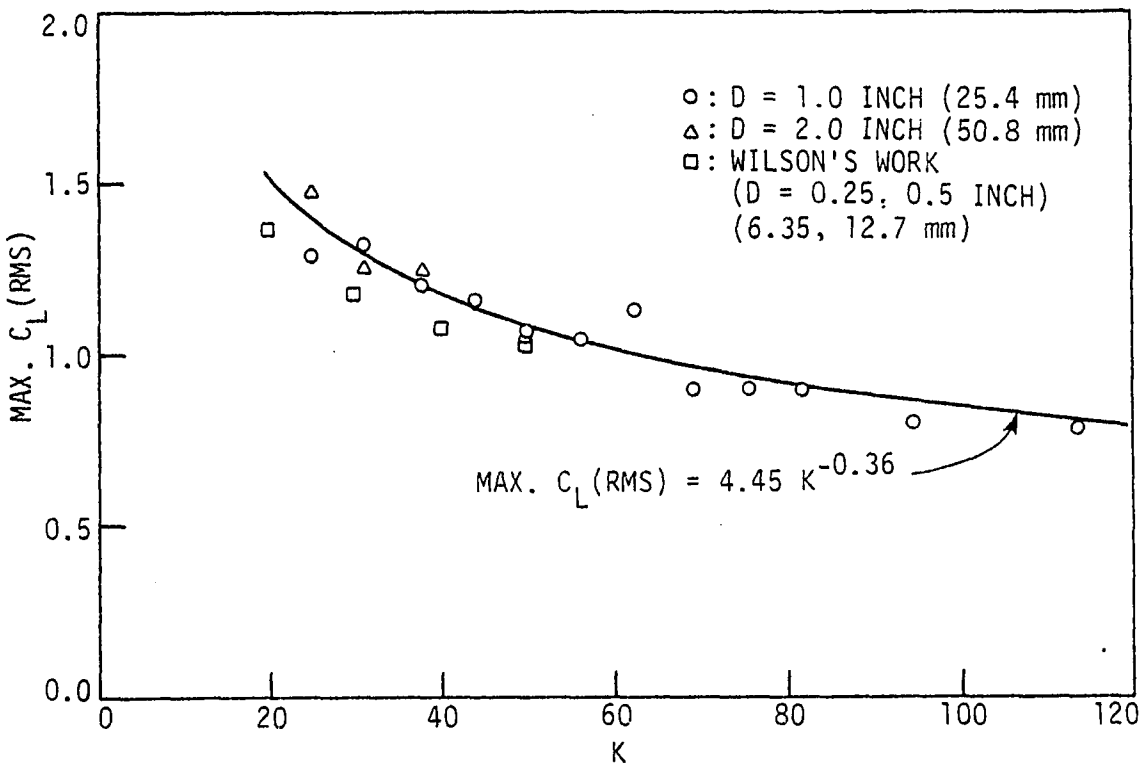

Figure 24. Maximum C_L(RMS) vs $K(=2\pi\frac{A}{D})$

VIII. BIBLIOGRAPHY

1. Morison, J. R., M. R. O'Brien, J. W. Johnson, and S. A. Schaaf. "The Forces Exerted by Surface Waves on Piles." Petroleum Transactions 189 (1950):149-154.

2. Sarpkaya, T. "Forces on Cylinders and Spheres in a Sinusoidally Oscillating Fluid." Trans. ASME Journal of Applied Mechanics 42 (1975):32-37.

3. Blevins, R. D. Flow Induced Vibration. New York, N.Y.: Van Nostrand Reinhold, Co., 1977.

4. Iwan, W. D. and R. D. Blevins. "A Model for Vortex-induced Oscillation of Structures." Trans. ASME Journal of Applied Mechanics 41 (1974):581-586.

5. Toebes, G. H. "The Unsteady Flow and Wake Near an Oscillating Cylinder." Trans. ASME Journal of Basic Engineering 91 (1969):493-505.

6. Blevins, R. D., and T. E. Burton. "Fluid Forces Induced by Vortex Shedding." Journal of Fluid Engineering 98 (1976):19-26.

7. Keulegan, G. H. and L. H. Carpenter. "Forces on Cylinders and Plates in an Oscillating Fluid." Journal of Research of the National Bureau of Standards 60, No. 5 (1958):423-440.

8. Sarpkaya, T. "Forces on Cylinders and Spheres in a Sinusoidally Oscillating Fluid. Trans. ASME Journal of Applied Mechanics 42, No. 1 (1975):32-37.

9. Sarpkaya, T. "Vortex Shedding and Resistance in Harmonic Flow About Smooth and Rough Circular Cylinders at High Reynolds Numbers." Naval Postgraduate School Paper No. NPS-59SL76021, (Feb. 1976).

10. Hamann, F. H. and C. Dalton. "The Forces on a Cylinder Oscillating Sinusoidally in Water." Trans. ASME Journal of Engineering Industry 93 (1971):1197-1202.

11. Garrison, C. J., J. B. Field, and M. D. May. "Drag and Inertia Forces on a cylinder in Periodic Flow." Proc. of ASCE Journal of the Waterway, Port, Coastal and Ocean Div. 103, No. WW2 (1977):193-204.

12. Bishop, R. E. D. and A. Y. Hassan. "The Lift and Drag Forces on a Circular Cylinder Oscillating in a Flowing Fluid." Proc. Roy. Soc. London 277, Series A (1964): 51-75.

13. Tanida, Y., A. Okajima, and Y. Watanabe. "Stability of a Circular Cylinder Oscillating in Uniform Flow or in a Wake." Journal of Fluid Mechanics 61, part 4 (1973):769-784.

14. Fung, Y. C. "Fluctuating Lift and Drag Acting on a Cylinder in a Flow at Supercritical Reynolds Numbers. Journal of the Aerospace Sciences 27 (1960):801-814.

15. Batham, J. P. "Pressure Distributions on Circular Cylinders of Critical Reynolds Numbers." Journal of Fluid Mechanics 57, part 2 (1973):209-228.

16. Griffin, O. M. and S. E. Ramberg. "On Vortex Strength and Drag in Bluff-body Wakes." Journal of Fluid Mechanics 69, part 4 (1975):721-728.

17. Sarpkaya, T. "Fluid Forces on Oscillating Cylinders." Proc. of ASCE Journal of the Waterway, Port, Coastal and Ocean Div. 104, No. WW4 (1978): 275-290.

18. King, R., M. J. Prosser, and D. J. Johns. "On Vortex Excitation of Model Piles in Water." Journal of Sound and Vibration 29 (1973):169-188.

19. Weaver, W. "Wind-induced Vibrations in Antenna Members." Proc. of ASCE Journal of Engineering Mechanics Div. 87, No. EM 1 (1961):141-163.

20. Silvio, D. G. "Self-controlled Vibration of Cylinder in Fluid Stream." Proc. of ASCE Journal of Engineering Mechanics Div. 95, No. EM 2 (1969): 374-361.

21. Griffin, O. M. "A Universal Strouhal Number for the 'Locking-on' of Vortex Shedding to the Vibrations of Bluff Cylinders." Journal of Fluid Mechanics 85, part 3 (1978):591-606.

22. Landl, R. "A Mathematical Model for Vortex-induced Vibrations of Bluff Bodies." Journal of Sound and Vibration 42 (1975):219-234.

23. Hartlen, R. T. and I. G. Currie. "Lift-oscillator Model of Vortex-induced Vibration." Proc. of ASCE Journal of Engineering Mechanics Div. 96, No. EM5 (1970):577-591.

24. Skop, R. A. and O. M. Griffin. "A Model for the Vortex-excited Resonant Vibrations of Bluff Bodies." Journal of Sound and Vibration 27 (1975):225-233.

25. Roshko, A. "On the Wake and Drag of Bluff Bodies." Journal of Aerospace Sciences 22, No. 2 (1955):124-132.

26. Stansby, P. K. "The Locking-on of Vortex Shedding Due to the Cross-stream Vibration of Circular Cylinders in Uniform and Shear Flows." Journal of Fluid Mechanics 74, part 4 (1976):641-665.

27. Koopman, G. H. "The Vortex of Vibrating Cylinders at Low Reynolds Numbers." Journal of Fluid Mechanics 28, part 3 (1967):501-512.

28. Griffin, O. H. "The Unsteady Wake of an Oscillating Cylinder at Low Reynolds Number." Trans. ASME Journal of Applied Mechanics 34 (1971):729-738.

29. Griffin, O. M. and S. E. Ramberg. "The Vortex-street Wakes of Vibrating Cylinders." Journal of Fluid Mechanics 66, part 3 (1974):553-576.

30. Griffin, O. M. and S. E. Ramberg. "Vortex Shedding from a Cylinder Vibrating in Line with an Incident Uniform Flow." Journal of Fluid Mechanics 75, part 2 (1976):257-272.

31. Ogawa, A. and K. Nakagawa. "Stability of the Vortex Street in the Wake of Stationary and Vibrating Cylinders." Trans. Japan Soc. Aero. Space Science 20, No. 50 (1978):167-176.

32. Bearman, P. W. "On Vortex-street Wakes." Journal of Fluid Mechanics 28 (1967):625-641.

33. Wiegel, R. L. Oceanographical Engineering. Englewood Cliffs, N.J.: Prentice-Hall, Inc., 1964.

34. Hogben, N. "Fluid Loading on Offshore Structures, a State of Art Appraisal: Wave Loads." The Royal Institution of Naval Architects, Maritime Technology Monograph, No. 1 (1974).

35. Grace. R. A. "Wave Forces on Submerged Objects." Univ. of Hawaii Lab-M-10, Miscellaneous Report No. 10 (July 1974).

36. Moe, G. and S. H. Crandall. "Extremes of Morison-type Wave Loading on a Single Pile." Trans. ASME Journal of Mechanical Design 100 (1978):100-104.

37. Laird, A. D. K., C. A. Johnson, and R. W. Walker. "Water Forces on Accelerated Cylinders." Proc. of ASCE Journal of the Waterways and Harbors Div., No. WWI (1959):99-119.

38. Bidde, D. D. "Laboratory Study of Lift Forces on Circular Piles." Proc. of ASCE Journal of the Waterways, Harbors and Coastal Engineering Div. 97, No. WW4 (1971):595-614.

39. Wilson, T. J. "Self-excited Vibration of a Cylinder Driven Sinusoidally in a Still Fluid." M.S. Thesis Iowa State University, Ames, Iowa (1977).

40. Park. Y. S. "Experimental Apparatus for Measuring Fluid Forces Acting on a Cylinder Driven Sinusoidally in Still Water." M.S. Thesis, Iowa State University, Ames, Iowa (1979).

41. Ericksson, L. E. and J. P. Reding. "Criterion for Vortex Periodicity in Cylinder Wakes." AIAA Journal 17, No. 19 (1979):1012-1013.

42. Isaacson, M. de St. O. "The Forces on Circular Cylinders in Waves." Ph.D. Thesis, University of Cambridge (1974).

43. Durgin, W. W., P. A. March, and P. J. Lefebvre. "Lower Mode Response of Circular Cylinders in Cross-flow." Journal of Fluids Engineering 102 (1980):183-190.

IX. ACKNOWLEDGMENTS

I would like to thank Dr. K. G. McConnell, my major professor, for his patient guidance during these years. It was a valuable experience gained by working under his supervision. I am indebted to him for many valuable suggestions and discussions regarding this research work. Also, I wish to thank Mr. T. Elliot for his assistance in the laboratory work.

I wish to thank my wife Kye-youn, who participated with me in those odd hours required for my study and research. Also I must thank my parents for their encouragement and understanding.

X. APPENDIX A: INERTIA FORCE ELIMINATION

In this experiment, a cylinder model was driven in a fluid at rest in order to generate a relative motion between the fluid and the cylinder model. In this situation, it is unavoidable that unwanted inertia forces, due to the cylinder oscillation, are added to the measured fluid forces. The unwanted inertia forces should be eliminated from the measured fluid forces in order to get pure fluid forces acting on a cylinder exposed to a periodic fluid flow.

This study developed a special technique in order to eliminate the unwanted inertia forces using two force transducers. The cylinder model and two force transducers were placed at Plate C as shown in Figure A1. Both Plate C and the cylinder translate with sinusoidal motion of $x = A \sin(\omega_d t)$ where x is the input or driving displacement, A is the amplitude of motion, ω_d is the angular frequency of oscillation, and t is time. The cylinder is attached to the Plate C through two flexures which provide stiff support normal to the page and soft support in the y-direction of motion.

Force transducer No. 1 (Sensotec Model LKAF-30) measures the resultant force acting on the cylinder in the direction of motion through a pretensioned wire.

The force measured by transducer No. 1 (F_1) is the sum of the fluid force acting on the cylinder (F_f) and the inertia force of the accelerating cylinder; i.e.

$$F_1 = F_f + M_s a \tag{A1}$$

where F_f is the fluid force, M_s is the cylinder mass, and a is the cylinder acceleration. The inertia force can be eliminated by using the second force transducer (Sensotec Model LKSA - 30) which measures only an inertia force from a small mass m subjected to the same acceleration a. An accelerometer can also be used to measure the signal that is proportional to the acceleration. The required signal is

$$F_2 = ma \tag{A2}$$

It is apparent that the inertia force $M_s a$ can be eliminated from Equation A1 by subtracting the appropriate amount of F_2; i.e.

$$F_f = F_1 - KF_2 = F_f + (M_s - Km)a \tag{A3}$$

The required subtraction can be obtained by electronic addition using linear operational amplifiers as outlined below.

The electronic voltage signal from force transducer No. 1 is given by

$$e_1 = K_1F_1 = K_1F_f + K_1M_s a \tag{A4}$$

and from force transudcer No. 2 by

$$e_2 = - K_2F_2 = -K_2ma \tag{A5}$$

where K_1 and K_2 represent the linear system scale factors. The minus sign in Equation A5 can be easily achieved by appropriate connections of the transducer. The resulting voltage is the sum of Equations (A4) and (A5) giving

$$e = e_1 + e_2 = K_1F_f + (K_1M_s - K_2m)a \tag{A6}$$

The scale factor K_2 is adjusted through experiment until the output voltage e is zero when the cylinder is freely oscillated in air instead of in water. Since K_1, M_s, and m are easily determined by weighing. It is rather simple to maintain the required cancellation relationship of

$$K_1M_s = K_2m \tag{A7}$$

The validity of this relationship is periodically checked through calibration procedures in which known resistors are shunted across one arm of the force transducer strain gage bridge. In order to check the effectiveness of this technique, the cylinder was driven in air and the corresponding three signals were recorded on the oscilloscope as shown in

Figure A2. The top signal is from the force transducer No. 1 and represents the inertia force of the cylinder. The lower signal is from the force transducer No. 2 and represents the acceleration of Plate C. The middle signal is the summation signal of both transducers. Assuming the fluid force in air driving is zero, the signal level of the force transducer No. 2 was adjusted with the middle signal becomes essentially zero. The scale sensitivity for the top and bottom signal was 0.5 volts/div. While that of the middle signal was 0.05 volts/div., so that the lack of cancellation is emphasized by a factor of 10. From results similar to Figure A2, it can be concluded that 97 per cent or more of the inertia force is compensated for and effectively removed from force signal F_1 using this technique.

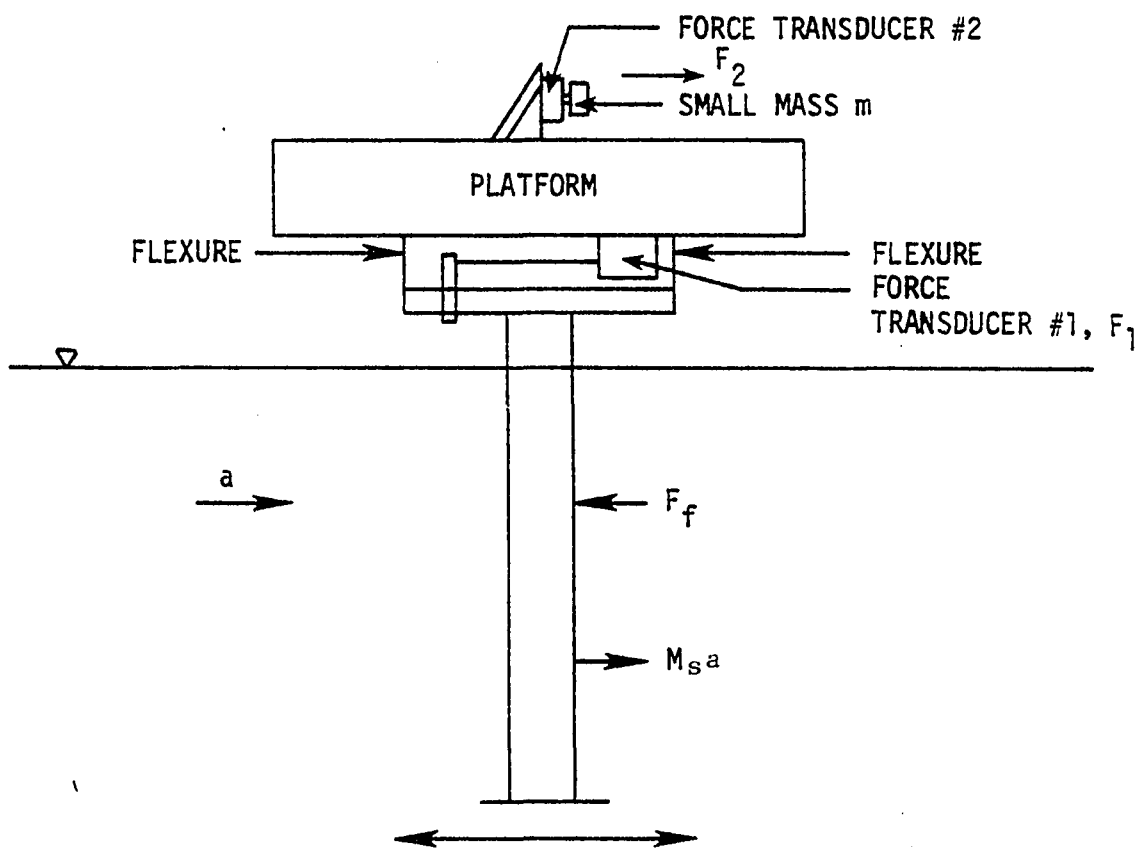

Figure A1. Force transducer locations in experimental apparatus

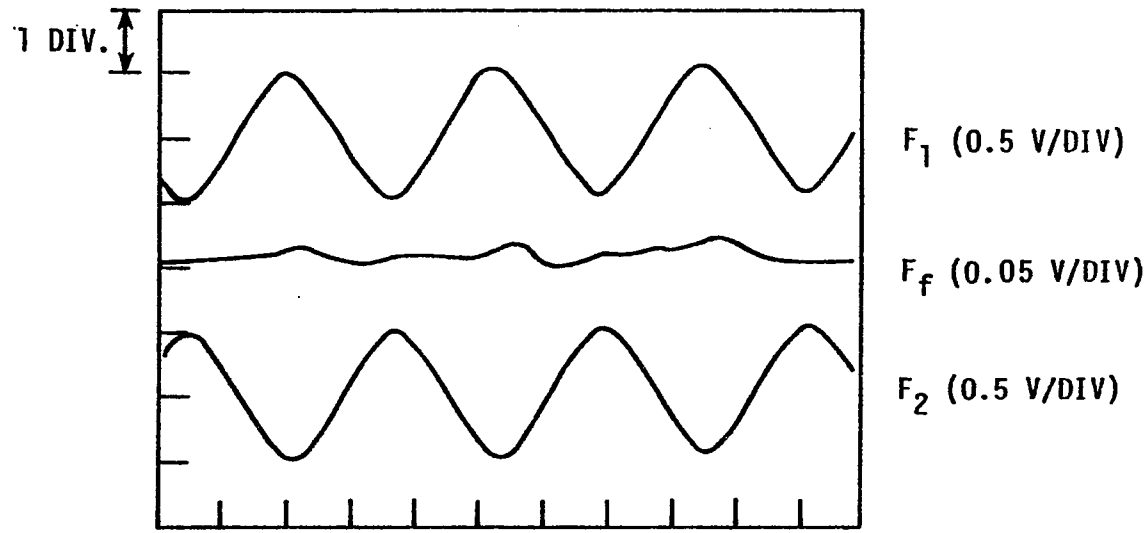

Figure A2. Comparison of measured cylinder inertia force and its compensation

XI. APPENDIX B: ELECTRONIC CIRCUITS USED

An amplifier and a second order low pass filter circuit were designed and built for the instrumentation used to detect and record the fluid forces and the cylinder responses in this experiment. Figure B1 shows a schematic diagram of the amplifier circuit used while Figure B2 shows that of the low pass filter circuit. These are standard analogue circuits described in many text books.

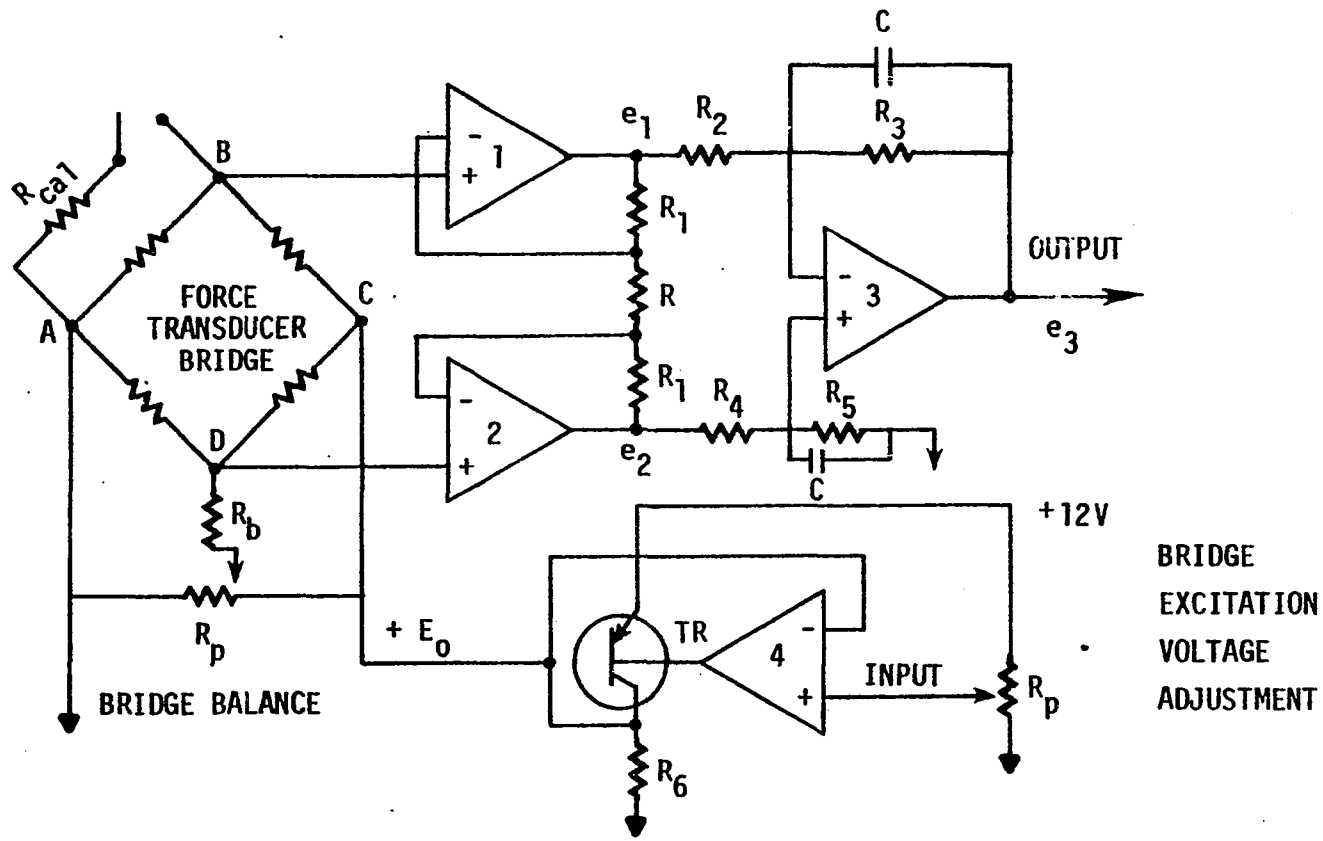

VALUES USED

R_{cal} = 249 k, R_b = 10 k, R_p = 100 k, R = 10 k, R_1 = 500 k, R_2 = 10 k, R_3 = 249 k, R_4 = 10 k, R_5 = 249 k, R_6 = 10 k, C = 0.001 µf

Figure B1. Schematic diagram of a used amplifier circuit

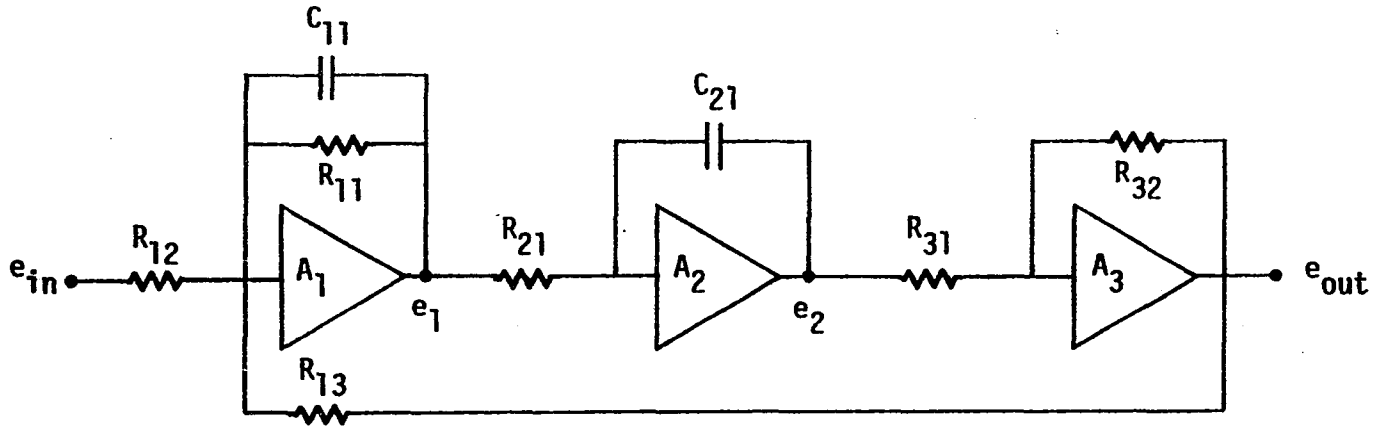

FOR f_n = 7 Hz and ζ = 0.65

$R_{12} = R_{13} = 0.20M$, $R_{11} = 0.175$ M, $R_{21} = 0.20$ M, $R_{31} = 0.1$ M,

$R_{32} = 0.077$ M, $C_{11} = 0.10$ µf, and $C_{21} = 0.10$ µf

Figure B2. Schematic diagram of a used second order low pass filter circuit

XII. APPENDIX C: PROGRAM USED IN NORLAND MODEL 3001

In order to effectively obtain all the useful frequency components of interest, a program was used in the Norland Model 3001 data analyzing unit. This program and the procedure to run the program are described below.

1. Program used

1) 0.05 == INCR
2) 0 == HSETP
3) 1023 == HSETQ
4) HSETP
5) HSETQ
6) PK-PK == R9
7) R9*0.5 == R9
8) COOR
9) V-R9 == R9
10) Q1-R9 == Q1
11) COOR
12) V*0.48077 == B (peak lift force in lb.)
13) HSETP
14) HSETQ
15) RMS == A
16) A*0.48077 == A (R.M.S. lift force in lb.)
17) PNEXT
18) QNEXT

19) PK-PK == R8

20) R8*0.5 == R8

21) COOR

22) V-R8 == R8

23) Q2-R8 == Q2

24) HSETP

25) HSETQ

26) PNEXT

27) QNEXT

28) RMS == B´

29) B´*0.51282 == B´ (R.M.S. cylinder response in inch)

30) R1*R1 == R2

31) R3*R3 == R4

32) R5/R7 == R6

33) R6*R2 == R6

34) R6*A == R0

35) R0/R4 == C (C_L (RMS))

36) R6*B == R0

37) R0/R4 == C´ (C_L(pk))

38) PSDQ1 == Q3

39) Q2 == Q1

40) PSDQ1 == Q2

41) DPLY A B B´ C C´ DPLY

42) GO TO 0.

2. Procedure to use the program.

   1) Connect the fluid lift force signal to channel 1 of the Norland and cylinder response signal to channel 2.

   2) Preset the cylinder driving amplitude (A, in inch) into registor R3 and the cylinder driving period (τ_d, in sec.) into registor R1 and the cylinder diameter (D, in inch) into registor R7.

   3) Preset a constant which will be used to calculate fluid lift force coefficients into registor R5. The constant can be calculated using Eqs. 19 and 20. When ℓ = 22 inch, and fluid density ρ = 1.937 slugs/ft^3, the constant was 24.651.

   4) Run the program.

   5) Read all the useful information from the Norland.